



HAL
open science

Anthropogenic-Biogenic Interactions at Night: Enhanced Formation of Secondary Aerosols and Particulate Nitrogen- and Sulfur-Containing Organics from beta-Pinene Oxidation

Li Xu, Zhaomin Yang, Narcisse Tsona, Xinke Wang, Christian George, Lin Du

► **To cite this version:**

Li Xu, Zhaomin Yang, Narcisse Tsona, Xinke Wang, Christian George, et al.. Anthropogenic-Biogenic Interactions at Night: Enhanced Formation of Secondary Aerosols and Particulate Nitrogen- and Sulfur-Containing Organics from beta-Pinene Oxidation. *Environmental Science and Technology*, 2021, 55 (12), pp.7794-7807. 10.1021/acs.est.0c07879 . hal-03300495

HAL Id: hal-03300495

<https://hal.science/hal-03300495v1>

Submitted on 6 Oct 2021

HAL is a multi-disciplinary open access archive for the deposit and dissemination of scientific research documents, whether they are published or not. The documents may come from teaching and research institutions in France or abroad, or from public or private research centers.

L'archive ouverte pluridisciplinaire **HAL**, est destinée au dépôt et à la diffusion de documents scientifiques de niveau recherche, publiés ou non, émanant des établissements d'enseignement et de recherche français ou étrangers, des laboratoires publics ou privés.



Distributed under a Creative Commons Attribution 4.0 International License

Anthropogenic–Biogenic Interactions at Night: Enhanced Formation of Secondary Aerosols and Particulate Nitrogen- and Sulfur-Containing Organics from β -Pinene Oxidation

Li Xu, Zhaomin Yang, Narcisse T. Tsona, Xinke Wang, Christian George, and Lin Du*

ABSTRACT: The oxidative photo-dehydrogenation of glycerol to produce H₂ and other valuable chemicals was studied using different materials. In particular, Pt nanoparticles were deposited on microemulsion-synthesized TiO₂ via surface organometallic chemistry (SOMC) and compared with photocatalysts obtained using more conventional methods. Well-defined Pt(II) single-site titania-grafted were prepared reacting the surface hydroxyl groups of TiO₂ nano-oxides with the organometallic Pt(COD)Me₂ complex. Sample reduction under H₂ generated ultrafine Pt nanoparticles well-dispersed on titania surface. Its performance under simulated solar light showed superior activity when compared to analogous Pt-containing catalysts prepared by other methods. Improved dispersion of Pt metal on titania surface was among the primary reasons of a better overall activity, providing relatively high rates of hydrogen productivity. Moreover, an increase of glyceraldehyde productivity in liquid phase was observed with the increase of Pt dispersion, demonstrating that the metal dispersion can strongly affect the selectivity of chemicals produced in the reaction. Comparison with state of the art shows that the present material exhibits excellent performance for a combined positive effect of the high specific surface area of titania prepared by microemulsion, giving access to the increased densities of active sites and the high dispersion of Pt nanoparticles given by the SOMC technique.

KEYWORDS: β -pinene, secondary aerosol, anthropogenic–biogenic interactions, organic nitrates, nitrooxy organosulfates, night time ozonolysis

1. INTRODUCTION

Aerosol particles in the atmosphere have negative impacts on regional air quality, climate change, and human health.^{1,2} Secondary aerosols produced during the oxidation of volatile organic compounds (VOCs) or inorganic precursors, for example, NO_x/SO₂/NH₃, represent a large fraction of the total aerosol particle mass.^{3,4} Biogenic VOCs (BVOCs) are globally the main precursors for the secondary organic aerosol (SOA) budget due to their relatively high emission rates (about ten times higher than anthropogenic VOCs) and high reactivity toward atmospheric major oxidants.^{5–7} When BVOCs mix with anthropogenic emissions, the oxidation of BVOCs and their SOA formation potential can be altered as highlighted by many field observations.^{8–12} However, anthropogenic–biogenic interactions during SOA formation are more complex than their current representation in models, and consequently, uncertainties in the predicted SOA budget might be induced.^{13–16}

Nitrogen-containing and sulfur-containing compounds derived from BVOCs are key species in biogenic SOA. They can form via anthropogenic–biogenic interactions as anthropogenic pollutants, for example, NO_x/SO₂/NH₃/sulfate can serve as precursors to their formation.^{17–19} NO_x may impact organic nitrates and total SOA formation by either influencing the local oxidation capacity, especially during night time through the NO₃ radicals or by facilitating the formation of condensable organic nitrates.^{20–22} Modeled or field-observed correlations between NO_x and biogenic SOA formation are however still elusive as the decrease in NO_x can either decrease or increase biogenic SOA formation.²³ Particulate organosulfates, which are usually formed through the reactions involving VOC oxidation products and acidic sulfate, could be a potential source of “missing SOA” that is not yet implemented in current atmospheric models.^{24,25} Indeed,

Table 1. Summary of Experimental Conditions

exp. no. ^a	[β -pinene] ₀ (ppb)	[O ₃] ₀ (ppb)	[NO ₂] ₀ (ppb)	[SO ₂] ₀ (ppb)	[NH ₃] ₀ (ppb)	T (K)	RH (%)	aerosol mass ($\mu\text{g m}^{-3}$)	aerosol yield
βO^b	154	624	0			300	22	156.4 \pm 2.9	0.18 \pm 0.01
$\beta\text{ON.1}$	154	567	32			298	33	290.8 \pm 12.4	0.33 \pm 0.01
$\beta\text{ON.2}$	154	575	78			298	37	524.4 \pm 13.5	0.60 \pm 0.03
$\beta\text{ON.3}$	154	606	116			299	29	711.3 \pm 18.6	0.82 \pm 0.05
$\beta\text{ON.4}^b$	154	596	141			299	29	762.3 \pm 20.6	0.87 \pm 0.05
$\beta\text{ON.5}$	156	564	347			300	31	1088.7 \pm 27.0	1.25 \pm 0.07
$\beta\text{OS.1}$	156	543		39		297	31	281.8 \pm 6.2	0.32 \pm 0.02
$\beta\text{OS.2}$	155	606		59		296	31	313.0 \pm 13.1	0.36 \pm 0.02
$\beta\text{OS.3}$	156	614		100		297	30	415.5 \pm 6.5	0.48 \pm 0.02
$\beta\text{OS.4}^b$	156	608		134		298	28	659.8 \pm 10.7	0.76 \pm 0.04
$\beta\text{OS.5}$	157	612		198		299	25	676.4 \pm 10.7	0.78 \pm 0.04
$\beta\text{OA.1}$	152	599			48	296	25	186.4 \pm 13.2	0.21 \pm 0.02
$\beta\text{OA.2}^b$	155	591			98	297	29	178.4 \pm 5.4	0.20 \pm 0.01
$\beta\text{OA.3}$	156	609			147	297	27	205.6 \pm 13.1	0.24 \pm 0.01
$\beta\text{OA.4}$	156	591			196	296	28	214.3 \pm 5.0	0.25 \pm 0.01
$\beta\text{ONS.1}$	155	615	78	104		297	25	597.0 \pm 17.0	0.68 \pm 0.04
$\beta\text{ONS.2}^b$	154	602	134	102		297	31	795.5 \pm 10.0	0.91 \pm 0.05
$\beta\text{OSA.1}$	156	550		103	49	296	30	437.1 \pm 7.1	0.50 \pm 0.03
$\beta\text{OSA.2}^b$	155	631		105	98	295	22	375.6 \pm 2.3	0.43 \pm 0.02
$\beta\text{OSA.3}$	151	551		108	190	297	29	323.5 \pm 11.8	0.37 \pm 0.02

^aAbbreviations in experimental codes represent the reactants introduced into the chamber; that is, “ β ” represents β -pinene, “O” represents ozone, “N” represents nitrogen dioxide, “S” represents sulfur dioxide, and “A” represents ammonia. The number represents experiments with the same reactants but different concentrations. ^bExperiments were repeated under comparable conditions (Table S2 in the Supporting Information) to collect aerosol particles for offline composition analysis by UPLC/Q-Exactive-Focus HRMS.

BVOC-derived organosulfates have been widely observed from clean to polluted regions.^{8,10,17,24,26,27} Nitrooxy organosulfates (NOSs), the formation of which is related to both NO_x and sulfates, could also be produced with some diurnal trends. While daytime photooxidation was proposed to be the dominant source of biogenic NOSs in south China and northwest Europe, the enhanced NOS formation at night in Beijing and northeastern Germany was attributed to NO₃ and sulfate chemistry.^{24,26–29} Understanding the precursors and formation pathways of these nitrogen- and sulfur-containing products not only requires field observations but also more laboratory experiments exploring BVOC oxidation and aerosol composition under various mixed conditions.

O₃ and NO₃ radicals are two main atmospheric oxidants at night and their relative dominance depends on the NO_x levels.³⁰ In contrast to “traditional” studies where biogenic SOA formation from either O₃ or NO₃ was investigated separately, some recent studies directly explored those processes in the presence of O_x (O₃ + NO₂). Different effects of NO₂ have been characterized for different precursors as increasing NO₂ decreased α -pinene SOA yield but increased β -pinene, limonene, and γ -terpinene SOA formation.^{31–34} Sulfates usually act as seeds to alter the SOA mass and composition.^{35–37} Some studies directly introduced SO₂ during BVOCs ozonolysis and showed that SO₂ enhanced limonene and α -cedrene SOA but had a minor effect on α -pinene SOA.^{38,39} Whether enhanced functionalization could compensate for the reduced oligomerization likely determines the SO₂ effects on final SOA yields.³⁸

NH₃ is another gaseous inorganic pollutant that has been observed to correlate well with the peak level of secondary particle pollution.^{40,41} Laboratory studies showed that NH₃ tended to enhance SOA mass yield of α -pinene and limonene ozonolysis by forming nitrogen-containing compounds, but no clear associations of NH₃ with isoprene SOA were

observed.^{42–46} It has been predicted that 50% reduction in NH₃ together with a 15% reduction in NO_x and SO₂ could result in a decrease of particulate matter by 11–17% in China.⁴⁷ While increasing attention has been paid to the synergistic effects of NH₃ with SO₂ or with NO₂ in the photooxidation of some anthropogenic VOCs, such interactions in biogenic particle formation should be further investigated.^{48–51}

β -pinene with a global annual emission rate of 18.9 Tg contributes to about 17% of monoterpene in the atmosphere.^{7,52} Its atmospheric abundance and exocyclic double bond make it a common representative of exocyclic monoterpenes.⁵³ The ozonolysis of β -pinene at night has been observed to have a significant contribution to nocturnal nucleation.^{54,55} In the present study, laboratory experiments were conducted to explore the effects of inorganic pollutants on aerosol formation initiated by nucleation during β -pinene ozonolysis in the absence of seed particles. First, we characterized particle formation when one single gas (NO₂, SO₂, or NH₃) and its mixtures (NO₂ and SO₂ or SO₂ and NH₃) were present in the reaction system. Then, the chemical compositions of β -pinene SOA formed under different conditions were analyzed by infrared spectroscopy and high-resolution mass spectrometry. Accordingly, formation pathways of the specific particulate products, including nitrogen- and sulfur-containing compounds, were proposed to further reveal the effects of NO₂, SO₂, and NH₃ on aerosol composition.

2. EXPERIMENTAL METHODS

2.1. Controlled Chamber Experiments. Aerosol particle formation during β -pinene ozonolysis under various conditions was studied in a 1 m³ Teflon chamber, which was suspended in a stainless-steel enclosure that enables dark conditions. Before the start of each experiment, the chamber was flushed with

purified, dried air until the background particle concentrations were lower than 10 cm^{-3} . Six groups of experiments were designed (Table 1). One group was pure β -pinene ozonolysis that was denoted as βO experiments. The other five groups that were performed with the presence of NO_2 , SO_2 , NH_3 , and the coexistence of NO_2 and SO_2 , SO_2 and NH_3 were coded as βON , βOS , βOA , βONS , and βOSA , respectively. The concentrations of β -pinene and O_3 in the experiments were higher than those in the real atmosphere to keep the particle production significant enough for accurate measurements while ratios of inorganic gases (NO_2 , SO_2 , NH_3) to O_3 and to β -pinene were in the range of 0–0.6 and 0–2.2, respectively. These ratios can partly represent relatively clean to relatively polluted atmospheric conditions, making comparisons between experimental conditions informative to aerosol generation in the atmosphere suffering different degrees of anthropogenic–biogenic interactions.^{15,55–62}

Experiments were carried out in three consecutive steps. The first step was the introduction of reactants into the chamber. First, β -pinene (Aladdin, >99%) and cyclohexane (Aladdin, >99%) with a concentration ratio of 1:220 were evaporated into the chamber by a flow of zero air. With such an excessive amount of cyclohexane, more than 95% of OH radicals formed from β -pinene ozonolysis were expected to be scavenged, giving the rate constants of OH reactions with β -pinene ($k_{\text{OH} + \beta\text{-pinene}} = 7.43 \times 10^{-11} \text{ cm}^3 \text{ molecule}^{-1} \text{ s}^{-1}$) and with cyclohexane ($k_{\text{OH} + \text{cyclohexane}} = 6.97 \times 10^{-12} \text{ cm}^3 \text{ molecule}^{-1} \text{ s}^{-1}$).⁶³ Subsequently, based on the experimental design, known amounts of NO_2 , SO_2 , and/or NH_3 stored in respective calibrated cylinders (490 ppm balanced in N_2 for NO_2 and NH_3 , 973 ppm balanced in N_2 for SO_2 , YuyanGas, China) were added into the chamber by flow controllers. Then, the chamber was allowed to equilibrate for about 20 min before the addition of ozone that started the reaction (i.e., reaction time = 0 min).

The second step was the particle formation and growth that lasted for about 3 h after the addition of O_3 . Particles were initially formed by homogeneous nucleation of products from β -pinene ozonolysis due to the lack of seed particles that would influence the particle composition. The initial amount of O_3 was 3–4 times higher than that of β -pinene, so that β -pinene could be consumed to a negligible level, as measured by a gas chromatograph coupled with a flame ionization detector (7890B, Agilent Technologies, USA) with a DB-624 capillary column (30 m \times 0.32 mm, 1.8 mm film thickness) when particle sampling started. During this period, particle size distribution, volume, and number concentrations were monitored continually by a scanning mobility particle sizer with a differential mobility analyzer (Model 3082, TSI Inc., USA) and a condensation particle counter (Model 3776, TSI Inc., USA). The mixing ratios of NO_2 and SO_2 were monitored by a $\text{NO}-\text{NO}_2-\text{NO}_x$ analyzer (model 42i, Thermo Scientific, USA) and SO_2 analyzer (model 43i, Thermo Scientific, USA), respectively. The concentration of NH_3 was not monitored and its initial concentration was obtained according to the volume of the chamber and its added amount. When the aerosol mass concentration stopped increasing, the experiment entered the third step where the generated aerosol particles were collected onto aluminum foil pieces by a 13-stage Dekati low-pressure impactor (DLPI+, DeKati Ltd, Finland) for offline chemical analysis. More detailed information about the particle measurement and sampling is provided in the Supporting Information.

2.2. Aerosol Yield Calculation and Correction. Aerosol yield (Y) is defined as the aerosol particle mass change (ΔM , $\mu\text{g m}^{-3}$) relative to the consumption of β -pinene ($\Delta[\beta\text{-pinene}]$, $\mu\text{g m}^{-3}$): $Y = \Delta M / \Delta[\beta\text{-pinene}]$. Aerosol particle mass concentrations were calculated based on the volume concentration measured by a scanning mobility particle sizer and the assumed 1.2 g cm^{-3} aerosol density.⁶⁴ Inorganic salts formed during β -pinene ozonolysis would increase aerosol density, hereby underestimating the aerosol yield by less than 8% in SO_2 -involved experiments when the density of inorganic salts was assumed to be 1.58 g cm^{-3} (see the Supporting Information).⁶⁵ The size-dependent wall loss rate of ammonium sulfate ($k_{\text{dp}} = 4.15 \times 10^{-7} \times D_p^{1.89} + 1.39 \times D_p^{-0.88}$, D_p is particle diameter in the unit of nm) was applied to the correction of particle mass concentration.⁶⁶ Details about this correction have been described in previous studies.^{34,67} Another factor that would influence the quantification of aerosol mass is the wall loss of organic vapors.^{68,69} Chamber walls and suspended particle surfaces compete for the deposition of organic vapors.⁷⁰ Accelerating reaction rates by employing an excessive amount of oxidant was reported to be one efficient way to suppress organic vapor wall loss because the fast formed particles could provide a significant sink for organic vapors to partition.^{36,53,71} The evaluation of the rate constants of vapor wall-loss and particle-loss in our reaction system indicates that organic vapors condensed to particles much faster than to the chamber walls (details are given in the Supporting Information). Therefore, the organic vapor wall loss has a minor effect on the SOA yield calculation and comparison.^{70,72}

2.3. Chemical Composition Characterization. To get details about the functional group and chemical bond information of particle-forming compounds, particles collected onto aluminum foil pieces were analyzed by an attenuated total reflectance coupled to a Fourier transform infrared spectrometer (Vertex 70, Bruker, Germany). It was operated with a scan resolution of 4 cm^{-1} for the spectral range of $4000\text{--}600 \text{ cm}^{-1}$. The spectra of blank aluminum foil pieces as backgrounds were subtracted from each sample measurement and the spectra baseline were corrected via the rubberband method (64 baseline points and 20 iterations).

Inorganic composition in secondary aerosol samples was further measured by means of ion chromatography (IC, Dionex ICS-600, Thermo Fisher, USA). Aluminum foil pieces were first dissolved in 4 mL of ultrapure water (Milli-Q, Millipore, France), followed by sonication for 30 min. Then, a Teflon membrane syringe filter (25 mm diameter, $0.22 \mu\text{m}$ pore, Jinteng, China) was used to remove insoluble species. Inorganic sulfate and ammonium in the prepared solution were measured with a Dionex IonPac CS12A analytical column (4 \times 250 mm) and Dionex IonPac AS19 analytical column (4 \times 250 mm) associated with their guard-column (4 \times 50 mm), respectively. The eluents were potassium hydroxide and methanesulfonic acid solutions, with a flow rate of 1.0 mL min^{-1} for the separation of anions and cations, respectively.

To further characterize the aerosol organic composition, aerosol samples formed under different conditions (Table S1) were prepared and analyzed by ultraperformance liquid chromatography (UPLC, Ultimate 3000, Thermo scientific, USA)/electrospray ionization Q-Exactive-Focus high-resolution mass spectrometry (ESI-Q-Exactive-Focus HRMS, Thermo Scientific, USA). Organic compounds in sample extracts (sample extraction procedures are provided in the

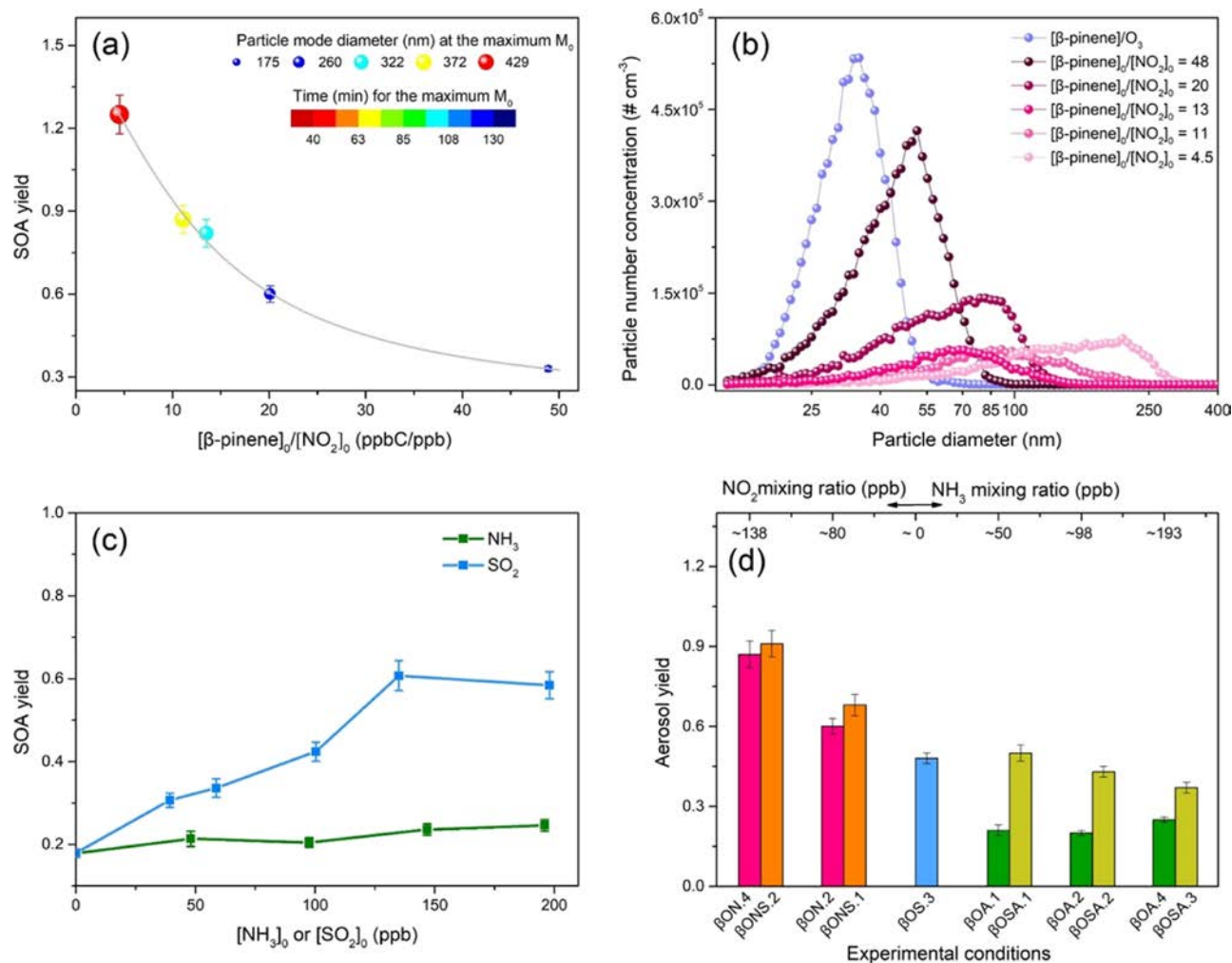


Figure 1. (a) SOA yield, particle mode diameter, and reaction time at the maximal SOA mass concentration (M_0) as a function of the $[\beta\text{-pinene}]_0/[\text{NO}_2]_0$ ratios. (b) Particle size distribution in the first 5 min of reactions with different $[\beta\text{-pinene}]_0/[\text{NO}_2]_0$ ratios. (c) SOA yield as a function of the initial mixing ratios of SO_2 ($[\text{SO}_2]_0$) and NH_3 ($[\text{NH}_3]_0$). (d) Comparison of the yield of aerosol formed in the presence of a single pollutant or mixed pollutants ($\text{NO}_2 + \text{SO}_2$ and $\text{SO}_2 + \text{NH}_3$). Experimental details are listed in Table 1.

Supporting Information) were separated using an Atlantis T3 C18 column (100 Å, 3 μm particle size, 2.1 mm \times 150 mm, Waters, USA). The mass spectrometer was operated in both negative and positive ionization modes with the mass range of m/z 50–750. Based on the full scan MS information, the most intense precursor ions were fragmented by a higher-energy collision-induced dissociation to get the MS/MS scan. The details about the chromatographic elution program and mass spectrometric parameters are described in the Supporting Information.

3. RESULTS AND DISCUSSION

3.1. NO_2 , SO_2 , and NH_3 Influenced β -Pinene SOA Formation. Experiments $\beta\text{ON.1}$ – 5 were designed to study the effects of initial NO_2 mixing ratios ($[\text{NO}_2]_0$) on β -pinene SOA formation. As shown in Figure 1a, the decrease in $[\beta\text{-pinene}]_0/[\text{NO}_2]_0$ (ppbC/ppb) ratios not only increased the SOA yield but also reduced the time for reaching the maximal aerosol mass concentration. Indeed, the particle size increase was accelerated by NO_2 after the onset of the reaction (Figure 1b). RH variation in these experiments may induce uncertainties in the particle growth and SOA yield, but the NO_2 enhancements in SOA formation can still be observed

when excluding one experiment ($\beta\text{ON.2}$) conducted under relatively high RH.^{73,74} Though NO_2 could perturb gas chemistry via its reaction with peroxy radicals, the thermally unstable peroxy nitrates are generally insignificant in SOA formation.^{75,76} NO_3 radicals, which could be quickly formed via $\text{NO}_2 + \text{O}_3$ reaction, are more likely to explain such an enhance NO_2 effect on particle formation rate and final mass due to its 5 orders of magnitude higher reactivity with β -pinene and higher SOA formation potential compared with β -pinene ozonolysis.^{33,77–80}

The enhanced β -pinene oxidation by NO_3 at high $[\text{NO}_2]_0$ and subsequent product (e.g., organic nitrates with low volatility) condensation and/or particle coagulation would grow particles to larger sizes.^{14,81,82} When the particle mass reached its maximum, as shown in Figure 1b, particle mode diameter (D_{pm}) was 109 nm with no NO_2 , while much larger particles were formed under higher $[\text{NO}_2]_0$ conditions (e.g., $D_{\text{pm}} = 429$ nm when $[\beta\text{-pinene}]_0/[\text{NO}_2]_0 = 4.5$). The enhanced SOA yields and particle size explained by NO_3 chemistry are supported by the results from previous studies, for which SOA yields of similar aerosol mass and D_{pm} in NO_3 -induced β -pinene oxidation ($Y = 1.34$, $D_{\text{pm}} = \sim 450$ nm) are comparable to those observed here.^{14,83} The much higher β -

pinene SOA formation potential at high NO_2 condition is consistent with model predictions in the area near Houston, where NO_3 oxidation of β -pinene alone was suggested to be the second-largest SOA source.⁸⁴ In many NO_x -polluted regions, enhanced night time SOA formation via NO_3 oxidation of monoterpenes has been demonstrated.^{16,18,19,26} Our results also suggest that β -pinene could be an important contributor to the enhanced SOA formation at night in these places with high anthropogenic NO_x emissions.

For β -pinene ozonolysis in experiments $\beta\text{OS.1-5}$, higher particle volume and number concentration as well as SOA yield (calculated by subtracting inorganic sulfate from the total aerosol as described in the Supporting Information and Table S2) were observed when $[\text{SO}_2]_0$ was high (Figures 1c and S1), in line with the previously reported role of SO_2 in the ozonolysis of limonene and butyl vinyl ether.^{38,66} The enhancement effect of SO_2 on SOA yield is smaller than that of NO_2 . For example, with similar initial β -pinene concentrations, the presence of 100 ppb SO_2 increased the SOA yield by 0.24 while 78 ppb NO_2 increased SOA yield by 0.42. Different from the direct competition between NO_3 and O_3 for β -pinene caused by NO_2 , one way for SO_2 to affect SOA formation is by reacting with stabilized Criegee intermediates (sCIs), forming SO_3 and finally sulfuric acid that is generally known to contribute to new particle formation and acid-catalyzed SOA formation.⁸⁵⁻⁸⁷ The formation of sulfate was confirmed by IC measurements. It is worth noting that the reaction between SO_2 and O_3 can be ruled out as the loss rates of SO_2 were comparable and negligible regardless of whether or not O_3 was present. The consumption of SO_2 increased with increasing $[\text{SO}_2]_0$ but decreased with $[\text{NO}_2]_0$ when NO_2 was also added (Figure S2). This is expected because the consumption of β -pinene by NO_3 that is derived from the $\text{NO}_2 + \text{O}_3$ reaction would lead to less sCI formation via β -pinene ozonolysis. Additionally, using formic acid (10 ppm) as the sCI scavenger in an additional experiment with similar reactant conditions to those of the $\beta\text{OS.2}$ experiment, the SO_2 consumption was nearly half compared to that in the absence of formic acid. This evidence suggests that the reaction between sCIs and SO_2 is an important sink of SO_2 , which has been proposed to be a significant source of atmospheric H_2SO_4 , especially in forest regions.⁸⁸⁻⁹⁰

The increased SO_2 consumption with increasing $[\text{SO}_2]_0$ leads to a linear ($R^2 = 0.97$) increase of the fraction of sulfate in enhanced aerosol mass (Figure S3). Considering that the hydrolysis of organosulfates during sample extraction may have a minor contribution to sulfate detected by IC, this fraction would be less than 0.4 when SO_2 decay reached 80 ppb. This significant difference suggests that besides the direct contribution of nucleated sulfate, other SO_2 -induced channels, such as the role of condensed sulfuric acid as seeds for capturing more SOA-forming vapors into the particle phase, acid-catalyzed heterogeneous reactions might also contribute to the enhanced particle formation.^{25,91-93}

SOA yields increased with NH_3 but the degree was much weaker than those of NO_2 and SO_2 (Figure 1c). The largest enhancement in SOA yield was observed to be 39% when the initial NH_3 mixing ratio approached 196 ppb. The maximal particle number concentration (N_{max}) and particle geometric mean diameter ($D_{\text{gm,max}}$) were also higher with NH_3 present (Figure S4d). These NH_3 effects on particle formation have also been reported during α -pinene and limonene ozonolysis.⁴²⁻⁴⁴ Ammonium salts of low volatility formed through the

gas-phase reaction between NH_3 and organic acids (e.g., pinic acid, pinonic acid, norpinic acid, and norpinonic acid) were suggested to account for the enhanced α -pinene/limonene SOA. The yield of organic acids was reported to be 4.2–17.2% of β -pinene + O_3 reactions and many of these organic acids can be produced during the α -pinene ozonolysis through similar reaction pathways.⁹⁴⁻⁹⁶ The vapor pressure of products from the $\text{NH}_3 +$ organic acid reaction were reported to be orders of magnitude lower than those of the corresponding acids.⁹⁷ Thus, it is expected that the acid–base reaction yielding condensable salts might be responsible for the enhanced β -pinene SOA formation in the presence of NH_3 .

3.2. Joint Effects of NO_2 and SO_2 on Secondary Aerosol Formation. As discussed above, the presence of NO_2 tends to produce larger particles with lower number concentrations, while SO_2 efficiently magnifies the particle number concentrations by forming relatively smaller particles. Mixed NO_2 and SO_2 seem to neutralize the single effect of NO_2 and SO_2 on particle formation, but SO_2 appears to be more effective in modifying particle size and number development. In the $\beta\text{ONS.1}$ experiment with $[\text{NO}_2]_0 = 78$ ppb, $[\text{SO}_2]_0 = 104$ ppb, the stabilized $D_{\text{gm,max}}$ at the end of the experiment was 67 nm lower than that in the $\beta\text{ON.2}$ case ($[\text{NO}_2]_0 = 78$ ppb) but only 15 nm larger than in $\beta\text{OS.3}$ case ($[\text{SO}_2]_0 = 100$ ppb) (Figure S4b,c,e). Compared to the βON experiments, the presence of SO_2 in the mixed $\text{NO}_2 + \text{SO}_2$ cases compensated for the reduction of N_{max} caused by NO_2 , making it at least 10 times higher in the latter than in the former case. Conversely, compared to the βOS experiments, the presence of NO_2 reduced N_{max} by about 0.8 times.

Unlike the neutralizing effects of NO_2 and SO_2 on the progression of particle size and number concentration, the coexistence of NO_2 and SO_2 shows a synergetic effect on the aerosol yield. As shown in Figure 1d, aerosol yields in βONS experiments were higher than in the corresponding βON or βOS experiments. The addition of NO_2 , on the one hand, introduces NO_3 , which could efficiently oxidize β -pinene and enhance SOA mass production. On the other hand, SO_2 consumption is reduced likely due to the suppressed sCI formation via β -pinene ozonolysis (Figure S2). However, certain amounts of SO_2 could still be oxidized and it is already efficient in modifying particle size distribution and number concentration. Hence, SO_2 -related enhanceive effects, such as promoting the generation of small particles that could act as condensation sinks and heterogeneous reactions may also assist the particle mass production, leading to a higher aerosol yield in βONS experiments than in βON experiments.

3.3. Joint Effects of SO_2 and NH_3 on Secondary Aerosol Formation. To study the combined effects of SO_2 and NH_3 on aerosol particle formation, three experiments were performed with $[\text{SO}_2]_0$ of about 110 ppb but varying $[\text{NH}_3]_0$ ($\beta\text{OSA.1-3}$). In these experiments, the increase of $[\text{NH}_3]_0$ led to a slight decrease of aerosol yields (Figure 1d). Interestingly, the aerosol yield in $\beta\text{OSA.1}$ ($[\text{SO}_2]_0 = 103$ ppb, $[\text{NH}_3]_0 = 49$ ppb) was a little higher than that of $\beta\text{OS.3}$ ($[\text{SO}_2]_0 = 100$ ppb). However, when $[\text{NH}_3]_0$ was elevated to 98 ppb or 190 ppb, the aerosol yields decreased and were lower than that in the $\beta\text{OS.3}$ experiment. The SO_2 consumptions in these experiments had a minor difference (Figure S2), suggesting the unlikelihood of NH_3 to directly change the fate of SO_2 . However, NH_3 would be absorbed onto the generated particles and acid–base neutralization reaction would occur between NH_3 and H_2SO_4 .^{49,98} The produced ammonium sulfate

(Figure S5) that could offer surface layers for condensation is crucial to particle formation.^{49,50,99,100} However, acid-related heterogeneous processes, which contribute to about 70% of the enhanced particle mass in the β OS.3 reaction, may be suppressed due to the neutralization reaction induced by NH_3 . Both the aerosol pH value (ranging from -2.5 to 1.2) modeled using the Extended Aerosol Inorganics Model (E-AIM model II, <http://www.aim.env.uea.ac.uk/aim/aim.php>) and the aerosol neutralization degree (0.4 – 0.9) calculated as the molar ratio of ammonium to sulfate ($[\text{NH}_4^+]/(2 \times [\text{SO}_4^{2-}])$) increased with $[\text{NH}_3]_0$ (see the Supporting Information).^{101,102} No clear correlation between liquid water contents calculated by E-AIM model II and initial NH_3 mixing ratios or aerosol yields could be observed. Therefore, the promoting effects derived from ammonium sulfate may not be enough to compensate for the mitigated acid catalytic effect and finally lead to the reduced aerosol yields with the increase of $[\text{NH}_3]_0$. It should be noted that ammonia depletion is not characterized by the appropriate instrument in the present study. Hence, more experiments are required to give deeper insights into the disturbed aerosol formation mechanism of β -pinene ozonolysis in the presence of both NH_3 and SO_2 .

3.4. Composition Analysis. **3.4.1. Identification of Functional Groups.** A typical set of infrared spectra of the particles formed under different conditions is shown in Figure 2, and the spectral assignment is summarized in Table S3.

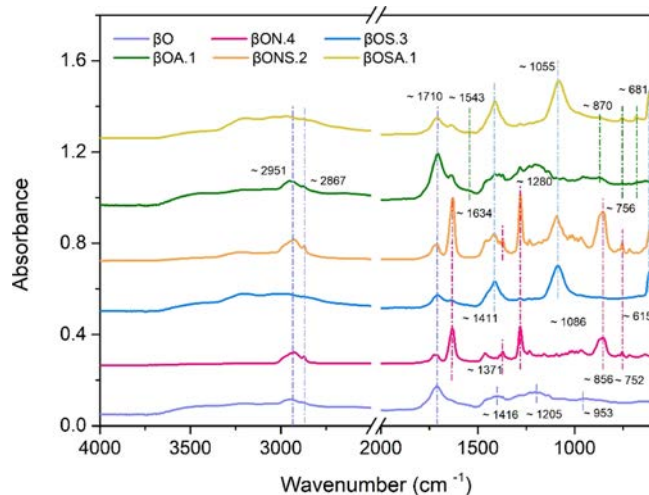


Figure 2. Infrared spectra of secondary aerosol particles generated from β -pinene ozonolysis under different experimental conditions. Experimental details are listed in Table 1.

When there were no inorganic gas pollutants present during β -pinene ozonolysis (β O), the main absorption band peaks were observed at approximately 1710 cm^{-1} , representing the stretching vibration of $\text{C}=\text{O}$ in carbonyl compounds.^{103,104} The absorbance in the 1490 – 1350 , 1335 – 1105 , and 990 – 820 cm^{-1} regions are the $\text{C}-\text{O}-\text{H}$ in plane bending (and/or $\text{C}-\text{H}$ bending), $\text{C}-\text{O}$ stretching, and $\text{O}-\text{H}$ deformation vibrations (and/or carboxylic $\text{C}-\text{O}-\text{H}$ out-of-plane bending), respectively.^{43,104–107} The broad bands range over 3680 – 3000 and 3000 – 2780 cm^{-1} are $\text{O}-\text{H}$ stretching in alcohols or acids and $\text{C}-\text{H}$ stretching absorption in the saturated carbon ring, respectively.¹⁰⁵

When NO_2 was added into β -pinene ozonolysis (β ON and β ONS), the formation of organic nitrates can be evidenced by the strong absorption bands at 1634 (NO_2 asymmetric stretching), 1281 (NO_2 symmetric stretching), and 856 cm^{-1} (NO symmetric stretching).^{76,108} The weak peak at 752 cm^{-1} also corresponds to organic nitrates.^{76,109} The dominant $\text{C}=\text{O}$ absorption in the β O experiment is replaced by organic nitrates. The presence of SO_2 induced new absorption bands located at 1412 , 1086 , and 615 cm^{-1} , which represent characteristic absorption of $\text{RO}-\text{SO}_2-\text{OR}'$ in organosulfates, symmetric $\text{S}-\text{O}$ stretching in organic or inorganic sulfates, and the absorption of inorganic sulfate, respectively.^{110–112} Both characteristic absorption peaks of organic nitrates and sulfates can be observed in β ONS experiments, consistent with NO_3 chemistry and sCl-induced sulfate chemistry discussed above. For aerosol particles formed in the presence of NH_3 , very weak absorption peaks featuring at 870 , 756 , and 681 cm^{-1} (Figure S6) likely match the vibrations of the $-\text{NH}_2$ group in the β OA experiment.^{106,113,114} The weaker IR absorption of nitrogen-containing species is somewhat in agreement with its slight SOA yield elevation, both of which indicate that NH_3 likely has a minor effect on particle-forming product generation. The coexistence of SO_2 and NH_3 introduced both sulfur-containing and nitrogen-containing compounds and the absorptions at 681 , 756 , and 1543 cm^{-1} ($\text{N}-\text{H}$ bending and/or $\text{C}-\text{N}$ stretching) were enhanced, indicating that the joint effect of SO_2 and NH_3 may occur in the β OSA experiment.

3.4.2. Identification of Nitrogen- and Sulfur-Containing Organic Compounds. The main identified particle-phase products in the series have been summarized in Table S4 and Figure 3. For single β -pinene ozonolysis (β O), a range of multifunctional products containing various combinations of carboxyl, carbonyl, and hydroxyl groups have been tentatively identified using high-resolution ESI (+) and/or ESI (–) mass spectrometry.⁹⁴ As shown in Figure S7, β -pinene ozonolysis occurs via the formation of a cyclic primary ozonide, the cycloreversion of which produces a C9-Criegee intermediate with formaldehyde and a C1-Criegee intermediate with nopinone, with the former channel being much more favored than the latter.^{94,96,115,116} The unimolecular reaction of the C9-Criegee intermediate via the hydroperoxide channel and the following series of radical reactions are responsible for the formation of the C8- and C9-monomers observed in the particle phase. In a previous study, organic acids, including pinic acid (MW = 186), pinalic-3-acid (MW = 170), and 4-hydroxypinonic-3-acid (MW = 186), have been observed in the early stage of β -pinene SOA growth.⁹⁶ These condensed acids were tentatively identified in the present study and they could partially explain the initial particle growth after the onset of the reaction.^{96,117} Dimers form another important set of nucleating agents for SOA particle formation.^{118,119} Reactions of sCIs with carbonyls to form secondary ozonides or with carboxylic acid to form peroxide ester and reactions between hydroperoxide and carbonyls to form peroxyhemiacetals (Figure S7) could account for a portion of dimer formation observed in the particle phase.^{120,121}

For aerosol particles generated from β -pinene ozonolysis in the presence of NO_2 , several organic nitrates were measured in positive ion mode as listed in Table S4. Their UPLC/Q-Exactive-Focus HRMS extracted ion chromatograms (EICs) are shown in Figure S8. Four organic nitrates [$\text{C}_{10}\text{H}_{17}\text{O}_4\text{N}$ (MW = 215), $\text{C}_{10}\text{H}_{15}\text{O}_5\text{N}$ (MW = 229), $\text{C}_{10}\text{H}_{17}\text{O}_5\text{N}$ (MW = 231), $\text{C}_{10}\text{H}_{15}\text{O}_6\text{N}$ (MW = 245)] were identified, following the

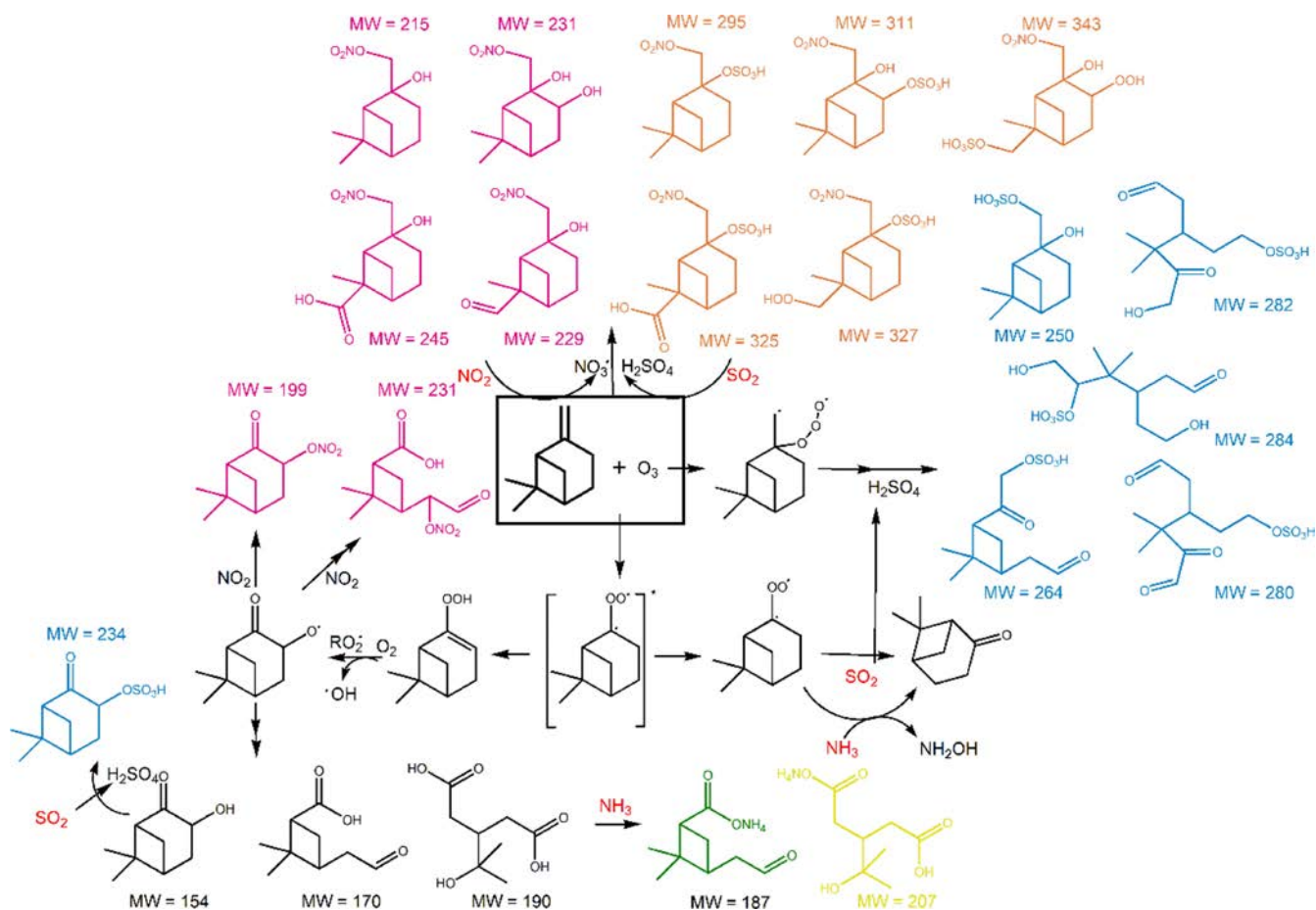


Figure 3. Summarized reaction scheme and products of β -pinene ozonolysis under different experimental conditions. For brevity, only one isomer of each compound is shown. Organic nitrates generated with the presence of NO_2 , organosulfates generated with the presence of SO_2 , nitroxy organosulfates generated with the coexistence of NO_2 and SO_2 , organic ammonium generated with the presence of NH_3 , and the coexistence of SO_2 and NH_3 are colored in pink, blue, orange, green, and yellow, respectively. Detailed potential formation mechanism for organic nitrates, organosulfates, and nitroxy organosulfates are provided in Figures S9 and S11.

NO_3 oxidation mechanisms proposed in the literature (Figure S9),^{14,122} consistent with our explanation that NO_2 increases the efficiency of β -pinene SOA production via its transformation to NO_3 . C10 compounds including those with the following chemical formulas, that is, $\text{C}_{10}\text{H}_{17}\text{O}_4\text{N}$, $\text{C}_{10}\text{H}_{15}\text{O}_5\text{N}$, and $\text{C}_{10}\text{H}_{17}\text{O}_5\text{N}$, have been observed in many ambient aerosol samples.^{20,56,57,123} Field observations showed that they account for more particle mass during night time than during daytime.^{20,22,56} The appearance of C10 organic nitrates in SOA samples produced under βON conditions illustrates that night time β -pinene oxidation can be one of their potential sources. Two C9 organic nitrates ($\text{C}_9\text{H}_{14}\text{O}_4\text{N}$ with MW = 199 and $\text{C}_9\text{H}_{13}\text{O}_6\text{N}$ with MW = 231) were also detected in positive ion mode. They might be produced via the reaction between NO_2 and reactive intermediates such as alkoxy radicals since NO_2 mixing ratios on the order of about 40 ppb were still present in the reaction mixture at the end of this experiment.^{124,125}

β -Pinene has been evidenced to be an important organosulfate precursor from both field and laboratory investigations.^{25,26,29,58,126} Acidic seed conditions are usually needed to transform β -pinene oxidation products to organosulfates through heterogeneous reactions.^{25,37,58,127} Though there were no acid seed particles added directly in the chamber during β -pinene ozonolysis, sulfuric acid produced via the

reaction of sCIs with SO_2 potentially created acidic conditions for some heterogeneous reactions. Organosulfates in aerosol particles from the βOS experiment were identified based on their exact masses (i.e., $\Delta M/M$ within ± 5 ppm) and the characteristic fragments of the sulfate group, including HSO_4^- (m/z 97), $^*\text{OSO}_3^-$ (m/z 96), HSO_3^- (m/z 81), and $^*\text{SO}_3^-$ (m/z 80), were shown in the high-resolution tandem MS/MS spectra. The EICs and MS/MS spectra for these organosulfates are displayed in Figure S10. Organosulfates detected as $[\text{M}-\text{H}]^-$ ions with m/z 249, 263, and 283 were identified to be $\text{C}_{10}\text{H}_{17}\text{O}_5\text{S}^-$, $\text{C}_{10}\text{H}_{15}\text{O}_6\text{S}^-$, and $\text{C}_{10}\text{H}_{19}\text{O}_7\text{S}^-$, respectively, consistent with those detected in particles generated from β -pinene ozonolysis in the presence of acidic sulfate seed particles.^{37,127} Ion formulas with m/z 279 and 281 were assigned to $\text{C}_{10}\text{H}_{17}\text{O}_7\text{S}^-$ and $\text{C}_{10}\text{H}_{19}\text{O}_7\text{S}^-$, respectively. They have been previously observed in aerosols generated from α -pinene, limonene, and α -terpinene oxidation and β -pinene photooxidation in the presence of acidic seeds.^{25,128} Indeed, all of these five organosulfates have a certain abundance in ambient particles collected from urban, forest, and marine regions in Asia, Europe, and the US.^{10,25,28,29,58,129} Our results demonstrate the potential contribution of β -pinene to these organosulfates, especially to $\text{C}_{10}\text{H}_{18}\text{O}_7\text{S}$ and $\text{C}_{10}\text{H}_{20}\text{O}_7\text{S}$ via the night time ozonolysis in the presence SO_2 . Besides the C10 organosulfates, two C9 compounds (m/z 233 and m/z 249)

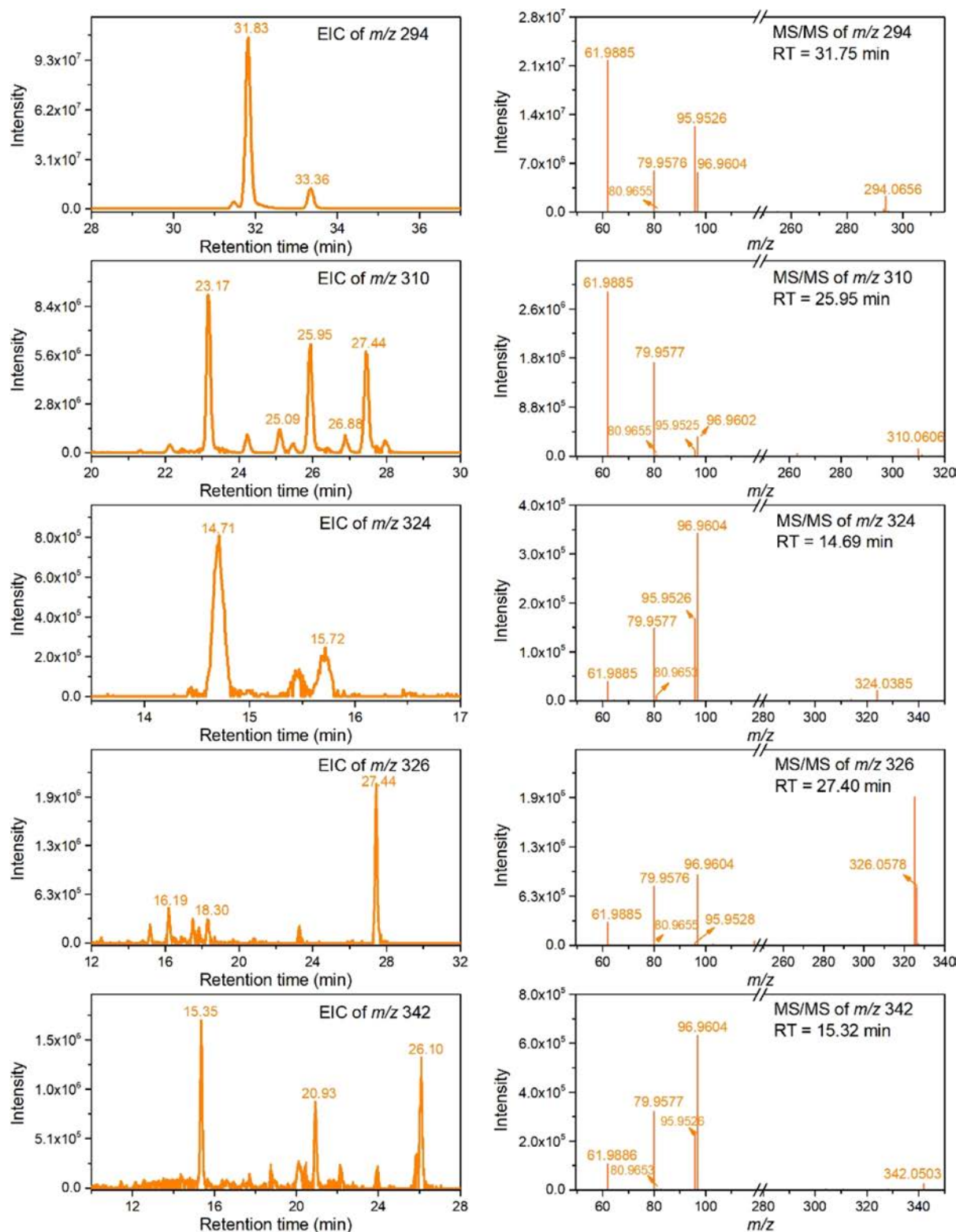


Figure 4. UPLC/Q₂-Exactive-Focus HRMS EICs and MS/MS spectra for *m/z* 294, 310, 324, 326, 342 ions (negative ion mode) in secondary aerosols generated from β -pinene ozonolysis with the coexistence of NO₂ and SO₂ (experimental details are listed in Table S2 in the Supporting Information). The maximal tolerance of mass error for all the precursor ions and product ions was set at 5 ppm.

were tentatively identified to organosulfates (C₉H₁₃O₅S⁻ and C₉H₁₃O₆S⁻, Figure S10). While the reaction between sulfuric acid and 3-hydroxynopinone that is generated from the Criegee channel might explain the formation of the

C₉H₁₃O₅S⁻ ion, the formation mechanism for C₉H₁₃O₆S⁻ is still unknown and needs to be further investigated.

The formation of the C₁₀ organosulfates suggests that some C₁₀ precursors, which could not be produced via the Criegee mechanism that leads to the fracture of the C₁₀ skeleton in β -

pinene to produce molecules containing less than nine carbons, should be produced through alternative reaction channels.^{29,37} As suggested in the literature, ozone tends to form an oxygen carbon σ -bond with one of the unsaturated carbon atoms of β -pinene (Figure S11). This σ -complex then undergoes decomposition, likely leading to a β -pinene oxide and myrtenol. While bicyclic organosulfates (m/z 249) are most likely formed through the direct attack of HSO_4^- on the protonated epoxide or its nucleophilic addition to the carbocation formed from the decomposition of protonated epoxide, a four-carbon ring-opened organosulfate (m/z 249) was also reported to derive from the rearranged carbocation.^{107,126,130,131} Myrtenol can be further oxidized by ozone and, after a series of reactions, finally produces some C10 compounds ($\text{C}_{10}\text{H}_{16}\text{O}_3$, $\text{C}_{10}\text{H}_{16}\text{O}_4$, $\text{C}_{10}\text{H}_{18}\text{O}_4$) containing the hydroxyl group. These C10 products can be detected in aerosol particles generated from the βO experiment in the absence of SO_2 in the present study and in the literature.³⁷ They possibly act as precursors for the formation of sulfate esters with m/z 263, 279, 281, 283 via the esterification reaction of the alcohol group with sulfuric acid.^{25,92,126}

When NO_2 and SO_2 were present during the reaction, five NOSs with m/z 294, 310, 324, 326, and 342 in negative ion mode were characterized. In addition to the extract mass of the parent NOSs ions, the prominent fragment ions from the sulfate group and product ions of NO_3^- (m/z 62) from a nitrooxy group can be observed in their MS/MS spectra (Figure 4), confirming the coexistence of nitrooxy and sulfate groups in their structures. Consequently, the $[\text{M} - \text{H}]^-$ ion formulas were $\text{C}_{10}\text{H}_{16}\text{NO}_7\text{S}^-$, $\text{C}_{10}\text{H}_{16}\text{NO}_8\text{S}^-$, $\text{C}_{10}\text{H}_{13}\text{NO}_9\text{S}^-$, $\text{C}_{10}\text{H}_{15}\text{NO}_9\text{S}^-$, and $\text{C}_{10}\text{H}_{16}\text{NO}_{10}\text{S}^-$ for m/z 294, 310, 324, 326, and 342, respectively. Apart from the m/z 324 compound that is observed for the first time in the present study, other four NOS ions could also be formed from β -pinene photooxidation in the presence of acidic seed particles.²⁵ With acidic seed particles, NO_3^- -initiated α -pinene oxidation was reported to produce NOSs ions at m/z 294 and 310.²⁵ In the present study, with the absence of acidic seed particles, NOSs are proposed to be formed via the NO_3^- -initiated β -pinene oxidation, followed by alcohol sulfate esterification reactions (Figure S9). These reaction pathways are expected because, as discussed above, NO_2 and SO_2 can influence the formation of NO_3^- and sulfuric acid. Not only these NOSs have been widely observed in ambient particles, but m/z 294, 310, 326 NOSs generally have higher concentrations at night as observed in Shanghai and Beijing (China), California (US), Antwerp (Belgium), K-puszta (Hungary), northeastern Bavaria (Germany).^{10,17,26,28,29,58,132–134} Our results suggest that interactions between β -pinene, O_3 , NO_2 , and SO_2 may enhance the formation of the five NOSs. Though the ratios of reactant concentrations used in the present study are comparable to that in the real atmosphere, whether or not these ambient NOSs could originate from β -pinene night time chemistry in addition to α -pinene NO_3^- -chemistry and monoterpene photooxidation in the presence of acidic sulfate particles should be further considered by a comprehensive analysis of specific atmospheric conditions. Future laboratory quantification of the yields of these nitrogen- and sulfur-containing products formed under typical atmospheric conditions is also needed to further illustrate their importance in the real atmosphere.

For NH_3 -involved β -pinene ozonolysis in the presence or absence of SO_2 , two organic ammonium carboxylates ($\text{C}_9\text{H}_{17}\text{O}_3\text{N}$ and $\text{C}_8\text{H}_{17}\text{O}_5\text{N}$) were tentatively identified and

their EICs are shown in Figure S12. These organic ammonium salts may be formed via the reaction between organic acids and NH_3 in the gas-phase, followed by the partition to the particle-phase, similar to the way of ammoniated product generation in NH_3 -involved α -pinene ozonolysis and photooxidation.^{42,45}

4. ATMOSPHERIC IMPLICATION

Currently, levels of O_3 and NH_3 in the atmosphere have been increasing over many regions of the earth.^{135,136} Though anthropogenic emissions of SO_2 and NO_2 have declined, their concentrations can still be above 100 ppb during severe haze pollution episodes.^{137,138} Anthropogenic–biogenic interactions occurring between β -pinene and these pollutants have been systematically investigated in the present study for the first time. It is demonstrated that NO_2 and SO_2 efficiently enhanced SOA formation, while NH_3 exhibited minor effects. The distinctly different responses of particle generation to mixed pollutants ($\text{SO}_2 + \text{NO}_2$ and $\text{SO}_2 + \text{NH}_3$) from that to the single one suggest that considering only the separate impacts of these pollutants likely induces bias prediction of secondary aerosol production. The observations here may be important for the accurate prediction of aerosol formation potential in regions with both anthropogenic and biogenic influences. The detection of particulate organic nitrates, organosulfates, as well as nitrooxy organosulfates pointed to the reaction channel leading to their formation even without any additional acidic seed particles. The increase of O_3 may further strengthen the importance of night time ozonolysis in the production of particulate nitrogen- and sulfur-containing compounds. These species have significant atmospheric impacts as organic nitrates could serve as permanent NO_x sinks to influence NO_x and O_3 cycling and organosulfates might affect the hygroscopicity of aerosol particles and cloud condensation nuclei properties.^{4,19,126} Though the naturally emitted BVOCs cannot be controlled directly, our results show that a fraction of biogenic SOA, such as these nitrogen- and sulfur-containing organics, can be controlled by mitigating anthropogenic pollutants, particularly NO_2 and SO_2 . Future research considering a better representation of chemically detailed anthropogenic–biogenic interactions in models is warranted to help to evaluate controllable SOA budget and reduce uncertainties in predicting the impacts of aerosol particles on air quality, climate, and human health.

ASSOCIATED CONTENT

Supporting Information

The Supporting Information is available free of charge at <https://pubs.acs.org/doi/10.1021/acs.est.0c07879>.

Additional experimental details; acidity calculation; assignment of ATR–FTIR absorption bands and compounds detected by UPLC/Q-Exactive-Focus HRMS; SO_2 consumption and particle size distribution under different experimental conditions; IC measurement of aerosol-phase sulfate and ammonium; UPLC/Q-Exactive-Focus HRMS EICs for organic nitrates, organosulfates, and organic ammonium; β -pinene ozonolysis and organic nitrates; and organosulfate formation mechanisms (PDF)

AUTHOR INFORMATION

Corresponding Author

Lin Du – Environment Research Institute, Shandong University, Qingdao 266237, China; orcid.org/0000-0001-8208-0558; Email: lindu@sdu.edu.cn

Authors

Li Xu – Environment Research Institute, Shandong University, Qingdao 266237, China; orcid.org/0000-0003-0573-9296

Zhaomin Yang – Environment Research Institute, Shandong University, Qingdao 266237, China

Narcisse T. Tsona – Environment Research Institute, Shandong University, Qingdao 266237, China; orcid.org/0000-0002-6023-1850

Xinke Wang – Université Lyon, Université Claude Bernard Lyon 1, CNRS, IRCELYON, F-69626 Villeurbanne, France

Christian George – School of Environmental Science and Engineering, Shandong University, Qingdao 266237, China; Université Lyon, Université Claude Bernard Lyon 1, CNRS, IRCELYON, F-69626 Villeurbanne, France; orcid.org/0000-0003-1578-7056

Notes

The authors declare no competing financial interest.

ACKNOWLEDGMENTS

This work was supported by the National Natural Science Foundation of China (91644214, 21876098), Youth Innovation Program of Universities in Shandong Province (2019KJD007), and Fundamental Research Fund of Shandong University (2020QNQT012). This project has received funding from the European Union's Horizon 2020 research and innovation program under grant agreement no 690958.

REFERENCES

- (1) Lelieveld, J.; Evans, J. S.; Fnais, M.; Giannadaki, D.; Pozzer, A. The contribution of outdoor air pollution sources to premature mortality on a global scale. *Nature* **2015**, *525*, 367–371.
- (2) Jimenez, J. L.; Canagaratna, M. R.; Donahue, N. M.; Prevot, A. S. H.; Zhang, Q.; Kroll, J. H.; DeCarlo, P. F.; Allan, J. D.; Coe, H.; Ng, N. L.; Aiken, A. C.; Docherty, K. S.; Ulbrich, I. M.; Grieshop, A. P.; Robinson, A. L.; Duplissy, J.; Smith, J. D.; Wilson, K. R.; Lanz, V. A.; Hueglin, C.; Sun, Y. L.; Tian, J.; Laaksonen, A.; Raatikainen, T.; Rautiainen, J.; Vaattovaara, P.; Ehn, M.; Kulmala, M.; Tomlinson, J. M.; Collins, D. R.; Cubison, M. J.; Dunlea, J.; Huffman, J. A.; Onasch, T. B.; Alfarra, M. R.; Williams, P. I.; Bower, K.; Kondo, Y.; Schneider, J.; Drewnick, F.; Borrmann, S.; Weimer, S.; Demerjian, K.; Salcedo, D.; Cottrell, L.; Griffin, R.; Takami, A.; Miyoshi, T.; Hatakeyama, S.; Shimono, A.; Sun, J. Y.; Zhang, Y. M.; Dzepina, K.; Kimmel, J. R.; Sueper, D.; Jayne, J. T.; Herndon, S. C.; Trimborn, A. M.; Williams, L. R.; Wood, E. C.; Middlebrook, A. M.; Kolb, C. E.; Baltensperger, U.; Worsnop, D. R. Evolution of organic aerosols in the atmosphere. *Science* **2009**, *326*, 1525–1529.
- (3) Dzepina, K.; Volkamer, R. M.; Madronich, S.; Tulet, P.; Ulbrich, I. M.; Zhang, Q.; Cappa, C. D.; Ziemann, P. J.; Jimenez, J. L. Evaluation of recently-proposed secondary organic aerosol models for a case study in Mexico City. *Atmos. Chem. Phys.* **2009**, *9*, 5681–5709.
- (4) Nah, T.; Sanchez, J.; Boyd, C. M.; Ng, N. L. Photochemical Aging of α -pinene and β -pinene Secondary Organic Aerosol formed from Nitrate Radical Oxidation. *Environ. Sci. Technol.* **2016**, *50*, 222–231.
- (5) Kanakidou, M.; Seinfeld, J. H.; Pandis, S. N.; Barnes, I.; Dentener, F. J.; Facchini, M. C.; Van Dingenen, R.; Ervens, B.; Nenes, A.; Nielsen, C. J.; Swietlicki, E.; Putaud, J. P.; Balkanski, Y.; Fuzzi, S.; Horth, J.; Moortgat, G. K.; Winterhalter, R.; Myhre, C. E. L.; Tsigaridis, K.; Vignati, E.; Stephanou, E. G.; Wilson, J. Organic aerosol and global climate modelling: A review. *Atmos. Chem. Phys.* **2005**, *5*, 1053–1123.
- (6) Guenther, A.; Hewitt, C. N.; Erickson, D.; Fall, R.; Geron, C.; Graedel, T.; Harley, P.; Klinger, L.; Lerdau, M.; McKay, W. A.; Pierce, T.; Scholes, B.; Steinbrecher, R.; Tallamraju, R.; Taylor, J.; Zimmerman, P. A global model of natural volatile organic compound emissions. *J. Geophys. Res. Atmos.* **1995**, *100*, 8873–8892.
- (7) Guenther, A. B.; Jiang, X.; Heald, C. L.; Sakulyanontvittaya, T.; Duhl, T.; Emmons, L. K.; Wang, X. The Model of Emissions of Gases and Aerosols from Nature version 2.1 (MEGAN2.1): an extended and updated framework for modeling biogenic emissions. *Geosci. Model Dev.* **2012**, *5*, 1471–1492.
- (8) Yee, L. D.; Isaacman-VanWertz, G.; Wernis, R. A.; Kreisberg, N. M.; Glasius, M.; Riva, M.; Surratt, J. D.; de Sá, S. S.; Alexander, M. L.; Palm, B. B.; Hu, W.; Campuzano-Jost, P.; Day, D. A.; Jimenez, J. L.; Liu, Y.; Misztal, P. K.; Artaxo, P.; Viegas, J.; Manzi, A.; de Souza, R. A. F.; Edgerton, E. S.; Baumann, K.; Goldstein, A. H.; Goldstein, A. H. Natural and anthropogenically influenced isoprene oxidation in southeastern United States and central Amazon. *Environ. Sci. Technol.* **2020**, *54*, 5980–5991.
- (9) Zhang, Y.-Q.; Chen, D.-H.; Ding, X.; Li, J.; Zhang, T.; Wang, J.-Q.; Cheng, Q.; Jiang, H.; Song, W.; Ou, Y.-B.; Ye, P.-L.; Zhang, G.; Wang, X.-M. Impact of anthropogenic emissions on biogenic secondary organic aerosol: Observation in the Pearl River Delta, southern China. *Atmos. Chem. Phys.* **2019**, *19*, 14403–14415.
- (10) Hettiyadura, A. P. S.; Al-Naiema, I. M.; Hughes, D. D.; Fang, T.; Stone, E. A. Organosulfates in Atlanta, Georgia: Anthropogenic influences on biogenic secondary organic aerosol formation. *Atmos. Chem. Phys.* **2019**, *19*, 3191–3206.
- (11) Shilling, J. E.; Zaveri, R. A.; Fast, J. D.; Kleinman, L.; Alexander, M. L.; Canagaratna, M. R.; Fortner, E.; Hubbe, J. M.; Jayne, J. T.; Sedlacek, A.; Setyan, A.; Springston, S.; Worsnop, D. R.; Zhang, Q. Enhanced SOA formation from mixed anthropogenic and biogenic emissions during the CARES campaign. *Atmos. Chem. Phys.* **2013**, *13*, 2091–2113.
- (12) Hoyle, C. R.; Boy, M.; Donahue, N. M.; Fry, J. L.; Glasius, M.; Guenther, A.; Hallar, A. G.; Huff Hartz, K.; Petters, M. D.; Petäjä, T.; Rosenoern, T.; Sullivan, A. P. A review of the anthropogenic influence on biogenic secondary organic aerosol. *Atmos. Chem. Phys.* **2011**, *11*, 321–343.
- (13) Shrivastava, M.; Cappa, C. D.; Fan, J.; Goldstein, A. H.; Guenther, A. B.; Jimenez, J. L.; Kuang, C.; Laskin, A.; Martin, S. T.; Ng, N. L.; Petaja, T.; Pierce, J. R.; Rasch, P. J.; Roldin, P.; Seinfeld, J. H.; Shilling, J.; Smith, J. N.; Thornton, J. A.; Volkamer, R.; Wang, J.; Worsnop, D. R.; Zaveri, R. A.; Zelenyuk, A.; Zhang, Q. Recent advances in understanding secondary organic aerosol: Implications for global climate forcing. *Rev. Geophys.* **2017**, *55*, 509–559.
- (14) Boyd, C. M.; Sanchez, J.; Xu, L.; Eugene, A. J.; Nah, T.; Tuet, W. Y.; Guzman, M. I.; Ng, N. L. Secondary organic aerosol formation from the β -pinene + NO₃ system: effect of humidity and peroxy radical fate. *Atmos. Chem. Phys.* **2015**, *15*, 7497–7522.
- (15) Nagori, J.; Janssen, R. H. H.; Fry, J. L.; Krol, M.; Jimenez, J. L.; Hu, W.; Vilà-Guerau de Arellano, J. Biogenic emissions and land-atmosphere interactions as drivers of the daytime evolution of secondary organic aerosol in the southeastern US. *Atmos. Chem. Phys.* **2019**, *19*, 701–729.
- (16) Xu, L.; Guo, H.; Boyd, C. M.; Klein, M.; Bougiatioti, A.; Cerully, K. M.; Hite, J. R.; Isaacman-VanWertz, G.; Kreisberg, N. M.; Knote, C.; Olson, K.; Koss, A.; Goldstein, A. H.; Hering, S. V.; de Gouw, J.; Baumann, K.; Lee, S.-H.; Nenes, A.; Weber, R. J.; Ng, N. L. Effects of anthropogenic emissions on aerosol formation from isoprene and monoterpenes in the southeastern United States. *Proc. Natl. Acad. Sci. U.S.A.* **2015**, *112*, 37–42.

- (17) Hettiyadura, A. P. S.; Jayarathne, T.; Baumann, K.; Goldstein, A. H.; de Gouw, J. A.; Koss, A.; Keutsch, F. N.; Skog, K.; Stone, E. A. Qualitative and quantitative analysis of atmospheric organosulfates in Centreville, Alabama. *Atmos. Chem. Phys.* **2017**, *17*, 1343–1359.
- (18) Kiendler-Scharr, A.; Mensah, A. A.; Friese, E.; Topping, D.; Nemitz, E.; Prevot, A. S. H.; Äijälä, M.; Allan, J.; Canonaco, F.; Canagaratna, M.; Carbone, S.; Crippa, M.; Dall'Osto, M.; Day, D. A.; De Carlo, P.; Di Marco, C. F.; Elbern, H.; Eriksson, A.; Freney, E.; Hao, L.; Herrmann, H.; Hildebrandt, L.; Hillamo, R.; Jimenez, J. L.; Laaksonen, A.; McFiggans, G.; Mohr, C.; O'Dowd, C.; Otjes, R.; Ovadnevaite, J.; Pandis, S. N.; Poulain, L.; Schlag, P.; Sellegri, K.; Swietlicki, E.; Tiitta, P.; Vermeulen, A.; Wahner, A.; Worsnop, D.; Wu, H.-C. Ubiquity of organic nitrates from nighttime chemistry in the European submicron aerosol. *Geophys. Res. Lett.* **2016**, *43*, 7735–7744.
- (19) Pye, H. O. T.; Luecken, D. J.; Xu, L.; Boyd, C. M.; Ng, N. L.; Baker, K. R.; Ayres, B. R.; Bash, J. O.; Baumann, K.; Carter, W. P. L.; Edgerton, E.; Fry, J. L.; Hutzell, W. T.; Schwede, D. B.; Shepson, P. B. Modeling the current and future roles of particulate organic nitrates in the Southeastern United States. *Environ. Sci. Technol.* **2015**, *49*, 14195–14203.
- (20) Huang, W.; Saathoff, H.; Shen, X.; Ramisetty, R.; Leisner, T.; Mohr, C. Chemical characterization of highly functionalized organonitrates contributing to night-time organic aerosol mass loadings and particle growth. *Environ. Sci. Technol.* **2019**, *53*, 1165–1174.
- (21) Sobanski, N.; Thieser, J.; Schuladen, J.; Sauvage, C.; Song, W.; Williams, J.; Lelieveld, J.; Crowley, J. N. Day and night-time formation of organic nitrates at a forested mountain site in south-west Germany. *Atmos. Chem. Phys.* **2017**, *17*, 4115–4130.
- (22) Yu, K.; Zhu, Q.; Du, K.; Huang, X.-F. Characterization of nighttime formation of particulate organic nitrates based on high-resolution aerosol mass spectrometry in an urban atmosphere in China. *Atmos. Chem. Phys.* **2019**, *19*, 5235–5249.
- (23) Liu, J.; Russell, L. M.; Ruggeri, G.; Takahama, S.; Claflin, M. S.; Ziemann, P. J.; Pye, H. O. T.; Murphy, B. N.; Xu, L.; Ng, N. L.; McKinney, K. A.; Budisulistiorini, S. H.; Bertram, T. H.; Nenes, A.; Surratt, J. D. Regional similarities and NO_x-related increases in biogenic secondary organic aerosol in summertime southeastern United States. *J. Geophys. Res. Atmos.* **2018**, *123*, 10620–10636.
- (24) Wang, Y.; Hu, M.; Wang, Y.-C.; Li, X.; Fang, X.; Tang, R.; Lu, S.; Wu, Y.; Guo, S.; Wu, Z.; Hallquist, M.; Yu, J. Z. Comparative Study of Particulate Organosulfates in Contrasting Atmospheric Environments: Field Evidence for the Significant Influence of Anthropogenic Sulfate and NO_x. *Environ. Sci. Technol. Lett.* **2020**, *7*, 787–794.
- (25) Surratt, J. D.; Gómez-González, Y.; Chan, A. W. H.; Vermeylen, R.; Shahgholi, M.; Kleindienst, T. E.; Edney, E. O.; Offenber, J. H.; Lewandowski, M.; Jaoui, M.; Maenhaut, W.; Claeys, M.; Flagan, R. C.; Seinfeld, J. H. Organosulfate formation in biogenic secondary organic aerosol. *J. Phys. Chem. A* **2008**, *112*, 8345–8378.
- (26) Wang, Y.; Hu, M.; Guo, S.; Wang, Y.; Zheng, J.; Yang, Y.; Zhu, W.; Tang, R.; Li, X.; Liu, Y.; Le Breton, M.; Du, Z.; Shang, D.; Wu, Y.; Wu, Z.; Song, Y.; Lou, S.; Hallquist, M.; Yu, J. The secondary formation of organosulfates under interactions between biogenic emissions and anthropogenic pollutants in summer in Beijing. *Atmos. Chem. Phys.* **2018**, *18*, 10693–10713.
- (27) He, Q.-F.; Ding, X.; Wang, X.-M.; Yu, J.-Z.; Fu, X.-X.; Liu, T.-Y.; Zhang, Z.; Xue, J.; Chen, D.-H.; Zhong, L.-J.; Donahue, N. M. Organosulfates from pinene and isoprene over the Pearl River Delta, South China: seasonal variation and implication in formation mechanisms. *Environ. Sci. Technol.* **2014**, *48*, 9236–9245.
- (28) Kristensen, K.; Glasius, M. Organosulfates and oxidation products from biogenic hydrocarbons in fine aerosols from a forest in North West Europe during spring. *Atmos. Environ.* **2011**, *45*, 4546–4556.
- (29) Iinuma, Y.; Müller, C.; Berndt, T.; Böge, O.; Claeys, M.; Herrmann, H. Evidence for the Existence of Organosulfates from β -Pinene Ozonolysis in Ambient Secondary Organic Aerosol. *Environ. Sci. Technol.* **2007**, *41*, 6678–6683.
- (30) Chen, X.; Wang, H.; Liu, Y.; Su, R.; Wang, H.; Lou, S.; Lu, K. Spatial characteristics of the nighttime oxidation capacity in the Yangtze River Delta, China. *Atmos. Environ.* **2019**, *208*, 150–157.
- (31) Perraud, V.; Bruns, E. A.; Ezell, M. J.; Johnson, S. N.; Yu, Y.; Alexander, M. L.; Zelenyuk, A.; Imre, D.; Chang, W. L.; Dabdub, D.; Pankow, J. F.; Finlayson-Pitts, B. J. Nonequilibrium atmospheric secondary organic aerosol formation and growth. *Proc. Natl. Acad. Sci. U.S.A.* **2012**, *109*, 2836–2841.
- (32) Presto, A. A.; Huff Hartz, K. E.; Donahue, N. M. Secondary organic aerosol production from terpene ozonolysis. 2. Effect of NO_x concentration. *Environ. Sci. Technol.* **2005**, *39*, 7046–7054.
- (33) Draper, D. C.; Farmer, D. K.; Desyaterik, Y.; Fry, J. L. A qualitative comparison of secondary organic aerosol yields and composition from ozonolysis of monoterpenes at varying concentrations of NO₂. *Atmos. Chem. Phys.* **2015**, *15*, 12267–12281.
- (34) Xu, L.; Tsona, N. T.; You, B.; Zhang, Y.; Wang, S.; Yang, Z.; Xue, L.; Du, L. NO_x enhances secondary organic aerosol formation from nighttime γ -terpinene ozonolysis. *Atmos. Environ.* **2020**, *225*, 117375.
- (35) Riva, M.; Budisulistiorini, S. H.; Zhang, Z.; Gold, A.; Surratt, J. D. Chemical characterization of secondary organic aerosol constituents from isoprene ozonolysis in the presence of acidic aerosol. *Atmos. Environ.* **2016**, *130*, 5–13.
- (36) Nah, T.; McVay, R. C.; Zhang, X.; Boyd, C. M.; Seinfeld, J. H.; Ng, N. L. Influence of seed aerosol surface area and oxidation rate on vapor wall deposition and SOA mass yields: a case study with α -pinene ozonolysis. *Atmos. Chem. Phys.* **2016**, *16*, 9361–9379.
- (37) Iinuma, Y.; Kahnt, A.; Mutzel, A.; Böge, O.; Herrmann, H. Ozone-driven secondary organic aerosol production chain. *Environ. Sci. Technol.* **2013**, *47*, 3639–3647.
- (38) Ye, J.; Abbatt, J. P. D.; Chan, A. W. H. Novel pathway of SO₂ oxidation in the atmosphere: Reactions with monoterpene ozonolysis intermediates and secondary organic aerosol. *Atmos. Chem. Phys.* **2018**, *18*, 5549–5565.
- (39) Yao, L.; Ma, Y.; Wang, L.; Zheng, J.; Khalizov, A.; Chen, M.; Zhou, Y.; Qi, L.; Cui, F. Role of stabilized Criegee Intermediate in secondary organic aerosol formation from the ozonolysis of α -cedrene. *Atmos. Environ.* **2014**, *94*, 448–457.
- (40) Ye, X.; Ma, Z.; Zhang, J.; Du, H.; Chen, J.; Chen, H.; Yang, X.; Gao, W.; Geng, F. Important role of ammonia on haze formation in Shanghai. *Environ. Res. Lett.* **2011**, *6*, 024019.
- (41) Wu, Y.; Gu, B.; Erisman, J. W.; Reis, S.; Fang, Y.; Lu, X.; Zhang, X. PM_{2.5} pollution is substantially affected by ammonia emissions in China. *Environ. Pollut.* **2016**, *218*, 86–94.
- (42) Na, K.; Song, C.; Switzer, C.; Cocker, D. R. Effect of Ammonia on Secondary Organic Aerosol Formation from α -Pinene Ozonolysis in Dry and Humid Conditions. *Environ. Sci. Technol.* **2007**, *41*, 6096–6102.
- (43) Babar, Z. B.; Park, J.-H.; Lim, H.-J. Influence of NH₃ on secondary organic aerosols from the ozonolysis and photooxidation of α -pinene in a flow reactor. *Atmos. Environ.* **2017**, *164*, 71–84.
- (44) Niu, X.; Ho, S. S. H.; Ho, K. F.; Huang, Y.; Cao, J.; Shen, Z.; Sun, J.; Wang, X.; Wang, Y.; Lee, S.; Huang, R. Indoor secondary organic aerosols formation from ozonolysis of monoterpene: An example of d-limonene with ammonia and potential impacts on pulmonary inflammations. *Sci. Total Environ.* **2017**, *579*, 212–220.
- (45) Hao, L.; Kari, E.; Leskinen, A.; Worsnop, D. R.; Virtanen, A. Direct contribution of ammonia to α -pinene secondary organic aerosol formation. *Atmos. Chem. Phys.* **2020**, *20*, 14393–14405.
- (46) Lin, Y.-H.; Knipping, E. M.; Edgerton, E. S.; Shaw, S. L.; Surratt, J. D. Investigating the influences of SO₂ and NH₃ levels on isoprene-derived secondary organic aerosol formation using conditional sampling approaches. *Atmos. Chem. Phys.* **2013**, *13*, 8457–8470.
- (47) Liu, M.; Huang, X.; Song, Y.; Tang, J.; Cao, J.; Zhang, X.; Zhang, Q.; Wang, S.; Xu, T.; Kang, L.; Cai, X.; Zhang, H.; Yang, F.; Wang, H.; Yu, J. Z.; Lau, A. K. H.; He, L.; Huang, X.; Duan, L.; Ding, A.; Xue, L.; Gao, J.; Liu, B.; Zhu, T. Ammonia emission control in China would mitigate haze pollution and nitrogen deposition, but worsen acid rain. *Proc. Natl. Acad. Sci. U.S.A.* **2019**, *116*, 7760–7765.

- (48) Qi, X.; Zhu, S.; Zhu, C.; Hu, J.; Lou, S.; Xu, L.; Dong, J.; Cheng, P. Smog chamber study of the effects of NO_x and NH₃ on the formation of secondary organic aerosols and optical properties from photo-oxidation of toluene. *Sci. Total Environ.* **2020**, *727*, 138632.
- (49) Jiang, X.; Lv, C.; You, B.; Liu, Z.; Wang, X.; Du, L. Joint impact of atmospheric SO₂ and NH₃ on the formation of nanoparticles from photo-oxidation of a typical biomass burning compound. *Environ. Sci. Nano* **2020**, *7*, 2532–2545.
- (50) Chen, T.; Liu, Y.; Ma, Q.; Chu, B.; Zhang, P.; Liu, C.; Liu, J.; He, H. Significant source of secondary aerosol: Formation from gasoline evaporative emissions in the presence of SO₂ and NH₃. *Atmos. Chem. Phys.* **2019**, *19*, 8063–8081.
- (51) Chu, B.; Zhang, X.; Liu, Y.; He, H.; Sun, Y.; Jiang, J.; Li, J.; Hao, J. Synergetic formation of secondary inorganic and organic aerosol: effect of SO₂ and NH₃ on particle formation and growth. *Atmos. Chem. Phys.* **2016**, *16*, 14219–14230.
- (52) Sindelarova, K.; Granier, C.; Bouarar, I.; Guenther, A.; Tilmes, S.; Stavrou, T.; Müller, J.-F.; Kuhn, U.; Stefani, P.; Knorr, W. Global data set of biogenic VOC emissions calculated by the MEGAN model over the last 30 years. *Atmos. Chem. Phys.* **2014**, *14*, 9317–9341.
- (53) Burkholder, J. B.; Baynard, T.; Ravishankara, A. R.; Lovejoy, E. R. Particle nucleation following the O₃ and OH initiated oxidation of α -pinene and β -pinene between 278 and 320 K. *J. Geophys. Res. Atmos.* **2007**, *112*, D10216.
- (54) Kammer, J.; Perraudin, E.; Flaud, P.-M.; Lamaud, E.; Bonnefond, J. M.; Villenave, E. Observation of nighttime new particle formation over the French Landes forest. *Sci. Total Environ.* **2018**, *621*, 1084–1092.
- (55) Kammer, J.; Flaud, P.-M.; Chazeaubeny, A.; Ciuraru, R.; Le Menach, K.; Geneste, E.; Budzinski, H.; Bonnefond, J. M.; Lamaud, E.; Perraudin, E.; Villenave, E. Biogenic volatile organic compounds (BVOCs) reactivity related to new particle formation (NPF) over the Landes forest. *Atmos. Res.* **2020**, *237*, 104869.
- (56) Lee, B. H.; Mohr, C.; Lopez-Hilfiker, F. D.; Lutz, A.; Hallquist, M.; Lee, L.; Romer, P.; Cohen, R. C.; Iyer, S.; Kurtén, T.; Hu, W.; Day, D. A.; Campuzano-Jost, P.; Jimenez, J. L.; Xu, L.; Ng, N. L.; Guo, H.; Weber, R. J.; Wild, R. J.; Brown, S. S.; Koss, A.; de Gouw, J.; Olson, K.; Goldstein, A. H.; Seco, R.; Kim, S.; McAvey, K.; Shepson, P. B.; Starn, T.; Baumann, K.; Edgerton, E. S.; Liu, J.; Shilling, J. E.; Miller, D. O.; Brune, W.; Schobesberger, S.; D'Ambro, E. L.; Thornton, J. A. Highly functionalized organic nitrates in the southeast United States: Contribution to secondary organic aerosol and reactive nitrogen budgets. *Proc. Natl. Acad. Sci. U.S.A.* **2016**, *113*, 1516–1521.
- (57) Ayres, B. R.; Allen, H. M.; Draper, D. C.; Brown, S. S.; Wild, R. J.; Jimenez, J. L.; Day, D. A.; Campuzano-Jost, P.; Hu, W.; de Gouw, J.; Koss, A.; Cohen, R. C.; Duffey, K. C.; Romer, P.; Baumann, K.; Edgerton, E.; Takahama, S.; Thornton, J. A.; Lee, B. H.; Lopez-Hilfiker, F. D.; Mohr, C.; Wennberg, P. O.; Nguyen, T. B.; Teng, A.; Goldstein, A. H.; Olson, K.; Fry, J. L. Organic nitrate aerosol formation via NO₃ + biogenic volatile organic compounds in the southeastern United States. *Atmos. Chem. Phys.* **2015**, *15*, 13377–13392.
- (58) Ma, Y.; Xu, X.; Song, W.; Geng, F.; Wang, L. Seasonal and diurnal variations of particulate organosulfates in urban Shanghai, China. *Atmos. Environ.* **2014**, *85*, 152–160.
- (59) Han, T.; Qiao, L.; Zhou, M.; Qu, Y.; Du, J.; Liu, X.; Lou, S.; Chen, C.; Wang, H.; Zhang, F.; Yu, Q.; Wu, Q. Chemical and optical properties of aerosols and their interrelationship in winter in the megacity Shanghai of China. *J. Environ. Sci.* **2015**, *27*, 59–69.
- (60) Wang, J.; Li, J.; Ye, J.; Zhao, J.; Wu, Y.; Hu, J.; Liu, D.; Nie, D.; Shen, F.; Huang, X.; Huang, D. D.; Ji, D.; Sun, X.; Xu, W.; Guo, J.; Song, S.; Qin, Y.; Liu, P.; Turner, J. R.; Lee, H. C.; Hwang, S.; Liao, H.; Martin, S. T.; Zhang, Q.; Chen, M.; Sun, Y.; Ge, X.; Jacob, D. J. Fast sulfate formation from oxidation of SO₂ by NO₂ and HONO observed in Beijing haze. *Nat. Commun.* **2020**, *11*, 2844.
- (61) Xu, L.; Suresh, S.; Guo, H.; Weber, R. J.; Ng, N. L. Aerosol characterization over the southeastern United States using high-resolution aerosol mass spectrometry: spatial and seasonal variation of aerosol composition and sources with a focus on organic nitrates. *Atmos. Chem. Phys.* **2015**, *15*, 7307–7336.
- (62) Edwards, P. M.; Aikin, K. C.; Dube, W. P.; Fry, J. L.; Gilman, J. B.; de Gouw, J. A.; Graus, M. G.; Hanisco, T. F.; Holloway, J.; Hübler, G.; Kaiser, J.; Keutsch, F. N.; Lerner, B. M.; Neuman, J. A.; Parrish, D. D.; Peischl, J.; Pollack, I. B.; Ravishankara, A. R.; Roberts, J. M.; Ryerson, T. B.; Trainer, M.; Veres, P. R.; Wolfe, G. M.; Warneke, C.; Brown, S. S. Transition from high- to low-NO_x control of night-time oxidation in the southeastern US. *Nat. Geosci.* **2017**, *10*, 490–495.
- (63) Atkinson, R.; Arey, J. Atmospheric degradation of volatile organic compounds. *Chem. Rev.* **2003**, *103*, 4605–4638.
- (64) Sarrafzadeh, M.; Wildt, J.; Pullinen, I.; Springer, M.; Kleist, E.; Tillmann, R.; Schmitt, S. H.; Wu, C.; Mentel, T. F.; Zhao, D.; Hastie, D. R.; Kiendler-Scharr, A. Impact of NO_x and OH on secondary organic aerosol formation from β -pinene photooxidation. *Atmos. Chem. Phys.* **2016**, *16*, 11237–11248.
- (65) Heym, C. Fluorescence histochemistry of biogenic monoamines. *Techniques in Neuroanatomical Research*; Springer, 1981; pp 139–170.
- (66) Zhang, P.; Chen, T.; Liu, J.; Liu, C.; Ma, J.; Ma, Q.; Chu, B.; He, H. Impacts of SO₂, relative humidity, and seed acidity on secondary organic aerosol formation in the ozonolysis of butyl vinyl ether. *Environ. Sci. Technol.* **2019**, *53*, 8845–8853.
- (67) Takekawa, H.; Minoura, H.; Yamazaki, S. Temperature dependence of secondary organic aerosol formation by photo-oxidation of hydrocarbons. *Atmos. Environ.* **2003**, *37*, 3413–3424.
- (68) Ye, P.; Ding, X.; Hakala, J.; Hofbauer, V.; Robinson, E. S.; Donahue, N. M. Vapor wall loss of semi-volatile organic compounds in a Teflon chamber. *Aerosol Sci. Technol.* **2016**, *50*, 822–834.
- (69) Zhang, X.; Cappa, C. D.; Jathar, S. H.; McVay, R. C.; Ensberg, J. J.; Kleeman, M. J.; Seinfeld, J. H. Influence of vapor wall loss in laboratory chambers on yields of secondary organic aerosol. *Proc. Natl. Acad. Sci. U.S.A.* **2014**, *111*, 5802–5807.
- (70) Zhang, X.; Schwantes, R. H.; McVay, R. C.; Lignell, H.; Coggon, M. M.; Flagan, R. C.; Seinfeld, J. H. Vapor wall deposition in Teflon chambers. *Atmos. Chem. Phys.* **2015**, *15*, 4197–4214.
- (71) Stirnweis, L.; Marcolli, C.; Dommen, J.; Barmet, P.; Frege, C.; Platt, S. M.; Bruns, E. A.; Krapf, M.; Slowik, J. G.; Wolf, R.; Prévôt, A. S. H.; Baltensperger, U.; El-Haddad, I. Assessing the influence of NO_x concentrations and relative humidity on secondary organic aerosol yields from α -pinene photo-oxidation through smog chamber experiments and modelling calculations. *Atmos. Chem. Phys.* **2017**, *17*, 5035–5061.
- (72) Matsunaga, A.; Ziemann, P. J. Gas-wall partitioning of organic compounds in a Teflon film chamber and potential effects on reaction product and aerosol yield measurements. *Aerosol Sci. Technol.* **2010**, *44*, 881–892.
- (73) Bonn, B.; Schuster, G.; Moortgat, G. K. Influence of water vapor on the process of new particle formation during monoterpene ozonolysis. *J. Phys. Chem. A* **2002**, *106*, 2869–2881.
- (74) Seinfeld, J. H.; Erdakos, G. B.; Asher, W. E.; Pankow, J. F. Modeling the formation of secondary organic aerosol (SOA). 2. The predicted effects of relative humidity on aerosol formation in the α -pinene-, β -pinene-, sabinene-, Δ^3 -carene-, and cyclohexene-ozone systems. *Environ. Sci. Technol.* **2001**, *35*, 1806–1817.
- (75) Atkinson, R. Gas-phase tropospheric chemistry of organic compounds: A review. *Atmos. Environ.* **2007**, *41*, 200–240.
- (76) Hallquist, M.; Wängberg, I.; Ljungström, E.; Barnes, I.; Becker, K.-H. Aerosol and product yields from NO₃ radical-initiated oxidation of selected monoterpenes. *Environ. Sci. Technol.* **1999**, *33*, 553–559.
- (77) Wang, H.; Chen, X.; Lu, K.; Hu, R.; Li, Z.; Wang, H.; Ma, X.; Yang, X.; Chen, S.; Dong, H.; Liu, Y.; Fang, X.; Zeng, L.; Hu, M.; Zhang, Y. NO₃ and N₂O₅ chemistry at a suburban site during the EXPLORE-YRD campaign in 2018. *Atmos. Environ.* **2020**, *224*, 117180.
- (78) Atkinson, R.; Hasegawa, D.; Aschmann, S. M. Rate constants for the gas-phase reactions of O₃ with a series of monoterpenes and related compounds at 296 ± 2 K. *Int. J. Chem. Kinet.* **1990**, *22*, 871–887.

- (79) Sander, S.; Abbatt, J.; Barker, J.; Burkholder, J.; Friedl, R.; Golden, D.; Huie, R.; Kolb, C.; Kurylo, M.; Moortgat, G. *Chemical Kinetics and Photochemical Data for Use in Atmospheric Studies, Evaluation Number 17*; JPL Publication, 2011; Vol. 10, pp 1–11.
- (80) Griffin, R. J.; Cocker, D. R.; Flagan, R. C.; Seinfeld, J. H. Organic aerosol formation from the oxidation of biogenic hydrocarbons. *J. Geophys. Res. Atmos.* **1999**, *104*, 3555–3567.
- (81) Coeur-Tourneur, C.; Tomas, A.; Guillebeau, A.; Henry, F.; Ledoux, F.; Visez, N.; Riffault, V.; Wenger, J. C.; Bedjanian, Y. Aerosol formation yields from the reaction of catechol with ozone. *Atmos. Environ.* **2009**, *43*, 2360–2365.
- (82) Fry, J. L.; Draper, D. C.; Barsanti, K. C.; Smith, J. N.; Ortega, J.; Winkler, P. M.; Lawler, M. J.; Brown, S. S.; Edwards, P. M.; Cohen, R. C.; Lee, L. Secondary organic aerosol formation and organic nitrate yield from NO₃ oxidation of biogenic hydrocarbons. *Environ. Sci. Technol.* **2014**, *48*, 11944–11953.
- (83) Bonn, B.; Moortgat, G. K. New particle formation during α - and β -pinene oxidation by O₃, OH and NO₃, and the influence of water vapour: particle size distribution studies. *Atmos. Chem. Phys.* **2002**, *2*, 183–196.
- (84) Russell, M. Predicting secondary organic aerosol formation rates in southeast Texas. *J. Geophys. Res.* **2005**, *110*, D07S17.
- (85) Sipilä, M.; Jokinen, T.; Berndt, T.; Richters, S.; Makkonen, R.; Donahue, N. M.; Mauldin III, R. L.; Kurtén, T.; Paasonen, P.; Sarnela, N.; Ehn, M.; Junninen, H.; Rissanen, M. P.; Thornton, J.; Stratmann, F.; Herrmann, H.; Worsnop, D. R.; Kulmala, M.; Kerminen, V.-M.; Petäjä, T. Reactivity of stabilized Criegee intermediates (sCIs) from isoprene and monoterpene ozonolysis toward SO₂ and organic acids. *Atmos. Chem. Phys.* **2014**, *14*, 12143–12153.
- (86) Jang, M.; Czoschke, N. M.; Lee, S.; Kamens, R. M. Heterogeneous atmospheric aerosol production by acid-catalyzed particle-phase reactions. *Science* **2002**, *298*, 814–817.
- (87) Sipilä, M.; Berndt, T.; Petaja, T.; Brus, D.; Vanhanen, J.; Stratmann, F.; Patokoski, J.; Mauldin, R. L., 3rd; Hyvarinen, A.-P.; Lihavainen, H.; Kulmala, M. The role of sulfuric acid in atmospheric nucleation. *Science* **2010**, *327*, 1243–1246.
- (88) Mauldin, R. L., III; Berndt, T.; Sipilä, M.; Paasonen, P.; Petäjä, T.; Kim, S.; Kurtén, T.; Stratmann, F.; Kerminen, V.-M.; Kulmala, M. A new atmospherically relevant oxidant of sulphur dioxide. *Nature* **2012**, *488*, 193–196.
- (89) Huang, H.-L.; Chao, W.; Lin, J. J.-M. Kinetics of a Criegee intermediate that would survive high humidity and may oxidize atmospheric SO₂. *Proc. Natl. Acad. Sci. U.S.A.* **2015**, *112*, 10857–10862.
- (90) Boy, M.; Mogensen, D.; Smolander, S.; Zhou, L.; Nieminen, T.; Paasonen, P.; Plass-Dülmer, C.; Sipilä, M.; Petäjä, T.; Mauldin, L.; Berresheim, H.; Kulmala, M. Oxidation of SO₂ by stabilized Criegee intermediate (sCI) radicals as a crucial source for atmospheric sulfuric acid concentrations. *Atmos. Chem. Phys.* **2013**, *13*, 3865–3879.
- (91) Stangl, C. M.; Krasnomowitz, J. M.; Apsokardu, M. J.; Tiszenkel, L.; Ouyang, Q.; Lee, S.; Johnston, M. V. Sulfur dioxide modifies aerosol particle formation and growth by ozonolysis of monoterpenes and isoprene. *J. Geophys. Res. Atmos.* **2019**, *124*, 4800–4811.
- (92) Iinuma, Y.; Müller, C.; Böge, O.; Gnauk, T.; Herrmann, H. The formation of organic sulfate esters in the limonene ozonolysis secondary organic aerosol (SOA) under acidic conditions. *Atmos. Environ.* **2007**, *41*, 5571–5583.
- (93) Zhang, P.; Chen, T.; Liu, J.; Chu, B.; Ma, Q.; Ma, J.; He, H. Impacts of mixed gaseous and particulate pollutants on secondary particle formation during ozonolysis of butyl vinyl ether. *Environ. Sci. Technol.* **2020**, *54*, 3909–3919.
- (94) Ma, Y.; Marston, G. Multifunctional acid formation from the gas-phase ozonolysis of β -pinene. *Phys. Chem. Chem. Phys.* **2008**, *10*, 6115–6126.
- (95) Yu, J.; Cocker, D. R., III; Griffin, R. J.; Flagan, R. C.; Seinfeld, J. H. Gas-phase ozone oxidation of monoterpenes: Gaseous and particulate products. *J. Atmos. Chem.* **1999**, *34*, 207–258.
- (96) Jaoui, M.; Kamens, R. M. Mass balance of gaseous and particulate products from β -pinene/O₃/air in the absence of light and β -pinene/NO₃/air in the presence of natural sunlight. *J. Atmos. Chem.* **2003**, *45*, 101–141.
- (97) Paciga, A. L.; Riipinen, I.; Pandis, S. N. Effect of ammonia on the volatility of organic diacids. *Environ. Sci. Technol.* **2014**, *48*, 13769–13775.
- (98) Liggio, J.; Li, S.-M.; Vlasenko, A.; Stroud, C.; Makar, P. Depression of ammonia uptake to sulfuric acid aerosols by competing uptake of ambient organic gases. *Environ. Sci. Technol.* **2011**, *45*, 2790–2796.
- (99) Zhang, R.; Khalizov, A.; Wang, L.; Hu, M.; Xu, W. Nucleation and growth of nanoparticles in the atmosphere. *Chem. Rev.* **2012**, *112*, 1957–2011.
- (100) Behera, S. N.; Sharma, M. Degradation of SO₂, NO₂ and NH₃ leading to formation of secondary inorganic aerosols: An environmental chamber study. *Atmos. Environ.* **2011**, *45*, 4015–4024.
- (101) Wexler, A. S.; Clegg, S. L. Atmospheric aerosol models for systems including the ions H⁺, NH₄⁺, Na⁺, SO₄²⁻, NO₃⁻, Cl⁻, Br⁻, and H₂O. *J. Geophys. Res. Atmos.* **2002**, *107*, ACH 14-1.
- (102) Engelhart, G. J.; Hildebrandt, L.; Kostenidou, E.; Mihalopoulos, N.; Donahue, N. M.; Pandis, S. N. Water content of aged aerosol. *Atmos. Chem. Phys.* **2011**, *11*, 911–920.
- (103) Sax, M.; Zenobi, R.; Baltensperger, U.; Kalberer, M. Time Resolved Infrared Spectroscopic Analysis of Aerosol Formed by Photo-Oxidation of 1,3,5-Trimethylbenzene and α -Pinene. *Aerosol Sci. Technol.* **2007**, *39*, 822–830.
- (104) Roberts, J. E.; Zeng, G.; Maron, M. K.; Mach, M.; Dwebi, I.; Liu, Y. Measuring heterogeneous reaction rates with ATR-FTIR spectroscopy to evaluate chemical fates in an atmospheric environment: A physical chemistry and environmental chemistry laboratory experiment. *J. Chem. Educ.* **2016**, *93*, 733–737.
- (105) Jia, L.; Xu, Y. Different roles of water in secondary organic aerosol formation from toluene and isoprene. *Atmos. Chem. Phys.* **2018**, *18*, 8137–8154.
- (106) Simons, W. W. *Sadtler Handbook of Infrared Spectra*; Sadtler Research Laboratories, 1978.
- (107) Lal, V.; Khalizov, A. F.; Lin, Y.; Galvan, M. D.; Connell, B. T.; Zhang, R. Heterogeneous reactions of epoxides in acidic media. *J. Phys. Chem. A* **2012**, *116*, 6078–6090.
- (108) Bruns, E. A.; Perraud, V.; Zelenyuk, A.; Ezell, M. J.; Johnson, S. N.; Yu, Y.; Imre, D.; Finlayson-Pitts, B. J.; Alexander, M. L. Comparison of FTIR and particle mass spectrometry for the measurement of particulate organic nitrates. *Environ. Sci. Technol.* **2010**, *44*, 1056–1061.
- (109) Day, D. A.; Liu, S.; Russell, L. M.; Ziemann, P. J. Organonitrate group concentrations in submicron particles with high nitrate and organic fractions in coastal southern California. *Atmos. Environ.* **2010**, *44*, 1970–1979.
- (110) Allen, D. T.; Palen, E. J.; Haimov, M. I.; Hering, S. V.; Young, J. R. Fourier Transform Infrared Spectroscopy of Aerosol Collected in a Low Pressure Impactor (LPI/FTIR): Method Development and Field Calibration. *Aerosol Sci. Technol.* **1994**, *21*, 325–342.
- (111) Coury, C.; Dillner, A. M. A method to quantify organic functional groups and inorganic compounds in ambient aerosols using attenuated total reflectance FTIR spectroscopy and multivariate chemometric techniques. *Atmos. Environ.* **2008**, *42*, 5923–5932.
- (112) Shen, P.; Zhang, H.; Zhang, S.; Fei, L. Fabrication of completely interface-engineered Ni(OH)₂/rGO nanoarchitectures for high-performance asymmetric supercapacitors. *Appl. Surf. Sci.* **2018**, *460*, 65–73.
- (113) Mohiuddin, K.; Strezov, V.; Nelson, P. F.; Evans, T. Bonding structure and mineral analysis of size resolved atmospheric particles nearby steelmaking industrial sites in Australia. *Aerosol Air Qual. Res.* **2016**, *16*, 1638–1650.
- (114) Liu, Y.; Liggio, J.; Staebler, R.; Li, S.-M. Reactive uptake of ammonia to secondary organic aerosols: Kinetics of organonitrogen formation. *Atmos. Chem. Phys.* **2015**, *15*, 13569–13584.

- (115) Ahrens, J.; Carlsson, P. T. M.; Hertl, N.; Olzmann, M.; Pfeifle, M.; Wolf, J. L.; Zeuch, T. Infrared Detection of Criegee Intermediates Formed during the Ozonolysis of β -Pinene and Their Reactivity towards Sulfur Dioxide. *Angew. Chem., Int. Ed.* **2014**, *53*, 715–719.
- (116) Carlsson, P. T. M.; Keunecke, C.; Krüger, B. C.; Maass, M.-C.; Zeuch, T. Sulfur dioxide oxidation induced mechanistic branching and particle formation during the ozonolysis of β -pinene and 2-butene. *Phys. Chem. Chem. Phys.* **2012**, *14*, 15637–15640.
- (117) Jenkin, M. E. Modelling the formation and composition of secondary organic aerosol from α - and β -pinene ozonolysis using MCM v3. *Atmos. Chem. Phys.* **2004**, *4*, 1741–1757.
- (118) Docherty, K. S.; Wu, W.; Lim, Y. B.; Ziemann, P. J. Contributions of organic peroxides to secondary aerosol formed from reactions of monoterpenes with O₃. *Environ. Sci. Technol.* **2005**, *39*, 4049–4059.
- (119) Heaton, K. J.; Dreyfus, M. A.; Wang, S.; Johnston, M. V. Oligomers in the early stage of biogenic secondary organic aerosol formation and growth. *Environ. Sci. Technol.* **2007**, *41*, 6129–6136.
- (120) Mackenzie-Rae, F. A.; Wallis, H. J.; Rickard, A. R.; Pereira, K. L.; Saunders, S. M.; Wang, X.; Hamilton, J. F. Ozonolysis of α -phellandrene – Part 2: Compositional analysis of secondary organic aerosol highlights the role of stabilised Criegee intermediates. *Atmos. Chem. Phys.* **2018**, *18*, 4673–4693.
- (121) Zhao, Z.; Xu, Q.; Yang, X.; Zhang, H. Heterogeneous ozonolysis of endocyclic unsaturated organic aerosol proxies: Implications for Criegee intermediate dynamics and later-generation reactions. *ACS Earth Space Chem.* **2019**, *3*, 344–356.
- (122) Ng, N. L.; Brown, S. S.; Archibald, A. T.; Atlas, E.; Cohen, R. C.; Crowley, J. N.; Day, D. A.; Donahue, N. M.; Fry, J. L.; Fuchs, H.; Griffin, R. J.; Guzman, M. I.; Herrmann, H.; Hodzic, A.; Iinuma, Y.; Jimenez, J. L.; Kiendler-Scharr, A.; Lee, B. H.; Luecken, D. J.; Mao, J.; McLaren, R.; Mutzel, A.; Osthoff, H. D.; Ouyang, B.; Picquet-Varrault, B.; Platt, U.; Pye, H. O. T.; Rudich, Y.; Schwantes, R. H.; Shiraiwa, M.; Stutz, J.; Thornton, J. A.; Tilgner, A.; Williams, B. J.; Zaveri, R. A. Nitrate radicals and biogenic volatile organic compounds: oxidation, mechanisms, and organic aerosol. *Atmos. Chem. Phys.* **2017**, *17*, 2103–2162.
- (123) Fisher, J. A.; Jacob, D. J.; Travis, K. R.; Kim, P. S.; Marais, E. A.; Chan Miller, C.; Yu, K.; Zhu, L.; Yantosca, R. M.; Sulprizio, M. P.; Mao, J.; Wennberg, P. O.; Crouse, J. D.; Teng, A. P.; Nguyen, T. B.; St Clair, J. M.; Cohen, R. C.; Romer, P.; Nault, B. A.; Wooldridge, P. J.; Jimenez, J. L.; Campuzano-Jost, P.; Day, D. A.; Hu, W.; Shepson, P. B.; Xiong, F.; Blake, D. R.; Goldstein, A. H.; Misztal, P. K.; Hainsco, T. F.; Wolfe, G. M.; Ryerson, T. B.; Wisthaler, A.; Mikoviny, T. Organic nitrate chemistry and its implications for nitrogen budgets in an isoprene- and monoterpene-rich atmosphere: constraints from aircraft (SEAC⁴RS) and ground-based (SOAS) observations in the Southeast US. *Atmos. Chem. Phys.* **2016**, *16*, 5969–5991.
- (124) Spittler, M.; Barnes, I.; Bejan, I.; Brockmann, K. J.; Benter, T.; Wirtz, K. Reactions of NO₃ radicals with limonene and α -pinene: Product and SOA formation. *Atmos. Environ.* **2006**, *40*, 116–127.
- (125) Gong, H.; Matsunaga, A.; Ziemann, P. J. Products and mechanism of secondary organic aerosol formation from reactions of linear alkenes with NO₃ radicals. *J. Phys. Chem. A* **2005**, *109*, 4312–4324.
- (126) Brüggemann, M.; Xu, R.; Tilgner, A.; Kwong, K. C.; Mutzel, A.; Poon, H. Y.; Otto, T.; Schaefer, T.; Poulain, L.; Chan, M. N.; Herrmann, H. Organosulfates in ambient aerosol: State of knowledge and future research directions on formation, abundance, fate, and importance. *Environ. Sci. Technol.* **2020**, *54*, 3767–3782.
- (127) Surratt, J. D.; Lewandowski, M.; Offenberg, J. H.; Jaoui, M.; Kleindienst, T. E.; Edney, E. O.; Seinfeld, J. H. Effect of acidity on secondary organic aerosol formation from isoprene. *Environ. Sci. Technol.* **2007**, *41*, 5363–5369.
- (128) Altieri, K. E.; Turpin, B. J.; Seitzinger, S. P. Oligomers, organosulfates, and nitroxy organosulfates in rainwater identified by ultra-high resolution electrospray ionization FT-ICR mass spectrometry. *Atmos. Chem. Phys.* **2008**, *9*, 2533–2542.
- (129) Stone, E. A.; Yang, L.; Yu, L. E.; Rupakheti, M. Characterization of organosulfates in atmospheric aerosols at Four Asian locations. *Atmos. Environ.* **2012**, *47*, 323–329.
- (130) Iinuma, Y.; Böge, O.; Kahnt, A.; Herrmann, H. Laboratory chamber studies on the formation of organosulfates from reactive uptake of monoterpene oxides. *Phys. Chem. Chem. Phys.* **2009**, *11*, 7985–7997.
- (131) Cortés, D. A.; Elrod, M. J. Kinetics of the Aqueous Phase Reactions of Atmospherically Relevant Monoterpene Epoxides. *J. Phys. Chem. A* **2017**, *121*, 9297–9305.
- (132) Gómez-González, Y.; Wang, W.; Vermeylen, R.; Chi, X.; Neiryneck, J.; Janssens, I. A.; Maenhaut, W.; Claeys, M. Chemical characterisation of atmospheric aerosols during a 2007 summer field campaign at Brasschaat, Belgium: Sources and source processes of biogenic secondary organic aerosol. *Atmos. Chem. Phys.* **2012**, *12*, 125–138.
- (133) Worton, D. R.; Goldstein, A. H.; Farmer, D. K.; Docherty, K. S.; Jimenez, J. L.; Gilman, J. B.; Kuster, W. C.; de Gouw, J.; Williams, B. J.; Kreisberg, N. M.; Hering, S. V.; Bench, G.; McKay, M.; Kristensen, K.; Glasius, M.; Surratt, J. D.; Seinfeld, J. H. Origins and composition of fine atmospheric carbonaceous aerosol in the Sierra Nevada Mountains, California. *Atmos. Chem. Phys.* **2011**, *11*, 10219–10241.
- (134) Gómez-González, Y.; Surratt, J. D.; Cuyckens, F.; Szmigielski, R.; Vermeylen, R.; Jaoui, M.; Lewandowski, M.; Offenberg, J. H.; Kleindienst, T. E.; Edney, E. O.; Blockhuys, F.; Van Alsenoy, C.; Maenhaut, W.; Claeys, M. Characterization of organosulfates from the photooxidation of isoprene and unsaturated fatty acids in ambient aerosol using liquid chromatography/(-) electrospray ionization mass spectrometry. *J. Mass Spectrom.* **2008**, *43*, 371–382.
- (135) Xu, X. Recent advances in studies of ozone pollution and impacts in China: A short review. *Curr. Opin. Environ. Sci. Health* **2021**, *19*, 100225.
- (136) Warner, J. X.; Dickerson, R. R.; Wei, Z.; Strow, L. L.; Wang, Y.; Liang, Q. Increased atmospheric ammonia over the world's major agricultural areas detected from space. *Geophys. Res. Lett.* **2017**, *44*, 2875–2884.
- (137) Liu, X. G.; Li, J.; Qu, Y.; Han, T.; Hou, L.; Gu, J.; Chen, C.; Yang, Y.; Liu, X.; Yang, T.; Zhang, Y.; Tian, H.; Hu, M. Formation and evolution mechanism of regional haze: a case study in the megacity Beijing, China. *Atmos. Chem. Phys.* **2013**, *13*, 4501–4514.
- (138) Li, H.; Zhang, Q.; Zhang, Q.; Chen, C.; Wang, L.; Wei, Z.; Zhou, S.; Parworth, C.; Zheng, B.; Canonaco, F.; Prévôt, A. S. H.; Chen, P.; Zhang, H.; Wallington, T. J.; He, K. Wintertime aerosol chemistry and haze evolution in an extremely polluted city of the North China Plain: significant contribution from coal and biomass combustion. *Atmos. Chem. Phys.* **2017**, *17*, 4751–4768.